

K16 AS A NOVEL REGULATOR OF NRF2 FUNCTION IN GLABROUS  
SKIN: IMPLICATIONS FOR PACHYONYCHIA CONGENITA  
AND ITS TREATMENT

by  
Rosemary G. Lu

A thesis submitted to Johns Hopkins University in conformity with the  
requirements for the degree of Master of Science

Baltimore, Maryland

August 2016

© 2016 Rosemary G. Lu  
All Rights Reserved

## ABSTRACT

The painful palmoplantar keratoderma (PPK) arising in individuals with pachyonychia congenita (PC) exhibit a significant upregulation of danger-associated molecular patterns and skin barrier regulators. Mice null for keratin 16 (*Krt16*), one of the genes mutated in PC, faithfully reproduce the morphological and molecular features of PC-associated PPK. We show here that onset of PPK is preceded by oxidative stress in male *Krt16*<sup>-/-</sup> mouse footpad skin, correlating with an inability of keratinocytes to sustain Nrf2-dependent expression of enzymes involved in the synthesis of the cellular antioxidant glutathione (GSH). Hypoactivity of Nrf2 coincides with impaired PKC $\delta$  activity and reduced levels of RACK1 protein in *Krt16*<sup>-/-</sup> footpad skin. Topical application of the small-molecule Nrf2 activator sulforaphane (SF) in male *Krt16*<sup>-/-</sup> mice prevents the development of PPK alongside a normalization of redox balance via the stimulation of GSH reductase and regeneration of GSH from existing cellular pools. Relative to males, female *Krt16*<sup>-/-</sup> mice exhibit faulty responsiveness to SF treatment. Preliminary data suggests that dual treatment of footpad skin with SF and selective estrogen receptor  $\beta$  agonist diarylpropionitrile (DPN) prevents the development of PPK lesions in female *Krt16*<sup>-/-</sup> mice. These findings point to oxidative stress and hypoactive Nrf2 as contributors to the pathogenesis of PC-related PPK and identify K16 as a regulator of the RACK1-PKC $\delta$ -NRF2 axis in skin keratinocytes. This pathway appears to be more complex in female *Krt16*<sup>-/-</sup> mice due to fundamental sex-based differences and, specifically, to a significant contribution of estrogen receptor signaling to modulation of Nrf2 function in skin keratinocytes. Our findings suggest a potential avenue to treat PC-associated PPK and may extend to similar keratin-based disorders.

## THESIS COMMITTEE

Dr. Pierre A. Coulombe and Dr. Michael J. Caterina

## ACKNOWLEDGEMENTS

I would first like to thank Dr. Pierre Coulombe for allowing me the opportunity to work in his laboratory and be part of not only a wonderful research team, but also such an amazing project. I have grown tremendously as an individual and a scientist, and I am extremely grateful for the training and intellectual stimulation over the past two years.

To Dr. Michael Caterina, for agreeing to be my secondary reader and offering great insight and suggestions for this thesis. It has also been a wonderful experience learning about the fascinating work being done in your laboratory during our joint lab meetings.

To Dr. Michelle Kerns, for her mentorship and teaching. Your guidance has taught me how to think scientifically and your ideas are inspiring. I am constantly pushed to perform better and rise to the occasion, and I am thankful to have worked on your team.

To Drs. Beau Su and Ryan Hobbs, for their generosity and scientific expertise in helping me navigate the laboratory, whether I encountered equipment issues or had questions regarding protocols and troubleshooting.

To the entire Coulombe laboratory, for creating a collegial and collaborative environment in which to work. Thank you for your critiques and suggestions during laboratory meetings and being supportive of my work and career goals.

To the BMB faculty and staff, thank you for creating a home away from home during my time at JHSPH. To Dr. Janice Evans, for advising me during my time in BMB on both academic and professional development. To Shannon Gaston, for guiding me through the logistics of my program and reminding me of deadlines when they slipped my mind.

To my family and friends, I cannot thank you enough for keeping me grounded and supporting my professional pursuits. For helping me through difficult times, being there to brighten my mood, and motivating me to push through, I am immensely grateful.

# TABLE OF CONTENTS

<b>Abstract</b>	ii
<b>Acknowledgements</b>	iii
<b>List of Figures</b>	vi
<b>List of Tables</b>	vii
<b>List of Abbreviations</b>	viii
<b>Introduction</b>	1
<i>Keratins</i>	1
<i>Pachyonychia congenita</i>	3
<i>Keratin 16 null mice: faithful model of pachyonychia congenita-associated palmoplantar</i>	4
<i>keratoderma</i>	
<i>Redox balance of the skin</i>	4
<i>Nrf2 signaling pathway as a regulator of redox balance</i>	6
<i>Estrogen signaling as a regulator of redox balance</i>	7
<b>Results</b>	10
<i>Impaired glutathione synthesis in pre-lesional male Krt16<sup>-/-</sup> front paw tissue</i>	10
<i>Lowering GSH levels causes PPK-like alterations in WT mouse skin</i>	10
<i>The transcription factor Nrf2 is expressed, but is hypoactive in pre-lesional</i>	12
<i>male Krt16<sup>-/-</sup> front paw skin</i>	
<i>Elucidating the link between Krt16 and Nrf2 activation</i>	13
<i>Small molecule-based activation of Nrf2 rescues PPK in male Krt16<sup>-/-</sup> mice</i>	15
<i>Topical treatment of Krt16<sup>-/-</sup> paws with SF exhibits sex-specific effects</i>	17
<i>Manipulation of ER signaling impacts responsiveness to SF treatment in</i>	18
<i>female Krt16<sup>-/-</sup> mice</i>	

<b>Discussion</b>	20
<b>Materials and Methods</b>	22
<b>Appendix I</b>	26
<b>References</b>	37
<b>Curriculum Vitae</b>	45

## LIST OF FIGURES

Figure 1. Keratin gene family tree.	1
Figure 2. Specificity of keratin expression in human epidermis.	2
Figure 3. Plantar skin of PC patient.	3
Figure 4. Schematic representation of GSH metabolism.	5
Figure 5. Schematic representation of KEAP1-NRF2 signaling pathway.	6
Figure 6. Decrease in GSH synthesis in male <i>Krt16</i> <sup>-/-</sup> pre-lesional paw skin enzymes.	10
Figure 7. Systemic BSO treatment results in increased oxidative burden and epidermal changes in male murine paw skin.	11
Figure 8. Impact of <i>Krt16</i> expression on Nrf2 activation.	12
Figure 9. A link between <i>Krt16</i> and Nrf2 activation.	14
Figure 10. Schematic of proposed regulation of Nrf2 pathway in the suprabasal epidermis under normal physiological conditions and without K16.	15
Figure 11. Treatment with SF prevents hyperkeratotic front paw calluses in <i>Krt16</i> <sup>-/-</sup> mice.	16
Figure 12. Topical treatment with SF results in increase of RACK1, PKCδ, and PKCδ-P.	17
Figure 13. Topical treatment of <i>Krt16</i> <sup>-/-</sup> paws with SF has sex-specific effects.	18
Figure 14. Manipulation of ER signaling impacts responsiveness to SF treatment in <i>Krt16</i> <sup>-/-</sup> female mice.	19

## LIST OF TABLES

Table 1. Characteristics of estrogen receptors.	8
Table 2. List of oligonucleotide primer sequences.	25

## LIST OF ABBREVIATIONS

ARE	Antioxidant responsive elements
BSO	L-buthionine-sulfoximine
C57BL/6	C57 black 6
DPN	Diarylpropionitrile
EBS	Epidermolysis bullosa simplex
ER	Estrogen receptor
G6PD	Glucose-6-phosphate dehydrogenase
GCL	Glutamate cysteine ligase
GCLC	Glutamate cysteine ligase catalytic subunit
GCLM	Glutamate cysteine ligase modulatory subunit
GS	Glutathione synthetase
GSH	Glutathione
GSR	Glutathione reductase
GSSG	Glutathione disulfide
GPX	Glutathione peroxidase
HO-1	Heme oxygenase 1
IPCC	International Pachyonychia Congenita Consortium
K1 or KRT1	Keratin 1
K5 or KRT5	Keratin 5
K6a or KRT6a	Keratin 6a
K6b or KRT6b	Keratin 6b
K10 or KRT10	Keratin 10
K14 or KRT14	Keratin 14

K16 or KRT16	Keratin 16
K17 or KRT17	Keratin 17
KEAP1	Kelch-like ECH-associating protein 1
ME1/2	Malic enzymes 1 and 2
NADPH	Nicotinamide adenine dinucleotide phosphate
NQO1	NAD(P)H dehydrogenase quinone 1
NRF2	Nuclear factor (erythroid-derived 2)-like 2
P21	Cyclin-dependent kinase inhibitor 1
PC	Pachyonychia congenita
PKC $\delta$	Protein kinase C delta
PPK	Palmoplantar keratoderma
RACK1	Receptor for activated C kinase 1
ROS	Reactive oxygen species
SF	Sulforaphane
SMAD2	Mothers against decapentaplegic homolog 2
TGF $\beta$	Transforming growth factor beta
WT	Wild-type

# INTRODUCTION

## *Keratins*

Keratins comprise the largest subgroup of intermediate filaments and function as the major structural proteins in epithelial cells (Coulombe and Omary, 2002). The keratin proteins can be grouped into two major types, type I or type II based on sequence homology (Figure 1), which co-assemble in an obligatory and pairwise fashion to form 10 nm filaments (Coulombe and Omary, 2002; Fuchs and Hanukoglu, 1983).

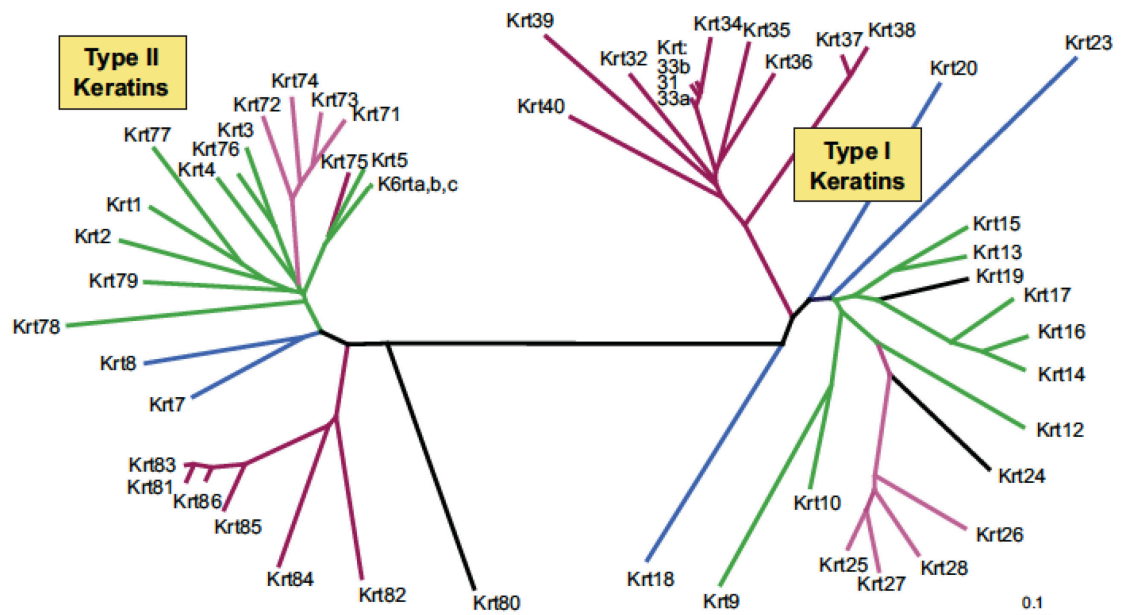


**Figure 1. Keratin gene family tree.** Keratins are grouped into Type I and Type II keratins (adapted from Coulombe, 2011).

Historically, the Coulombe laboratory has referred to keratins 6a/b (K6a/b), keratin 16 (K16), and keratin 17 (K17) as the wound repair-associated keratins (Paladini et al., 1996). The genes encoding for type II K6a/b and type I K16 and K17 are constitutively expressed in the epidermis of glabrous (hairless) skin and in all ectoderm-derived skin epithelial appendages (e.g., hair, nail, glands, tooth, thymus, etc.; Paladini et al., 1996). Expression of *KRT6a*, *KRT6b*,

*KRT16*, and *KRT17* are normally absent from interfollicular epidermis (and several related stratified epithelia) but are robustly induced following various types of insults, including UV exposure, wounding, and chronic inflammatory disease (McGowan and Coulombe, 1998). Upon wounding, K6a, K6b, K16, and K17 assume the spatial niche of the keratin 1 and keratin 10 (K1 and K10) pairing, which is normally expressed in the differentiating suprabasal layer of the epidermis (Figure 2; Fuchs and Green, 1980; Woodcock-Mitchell et al., 1982).

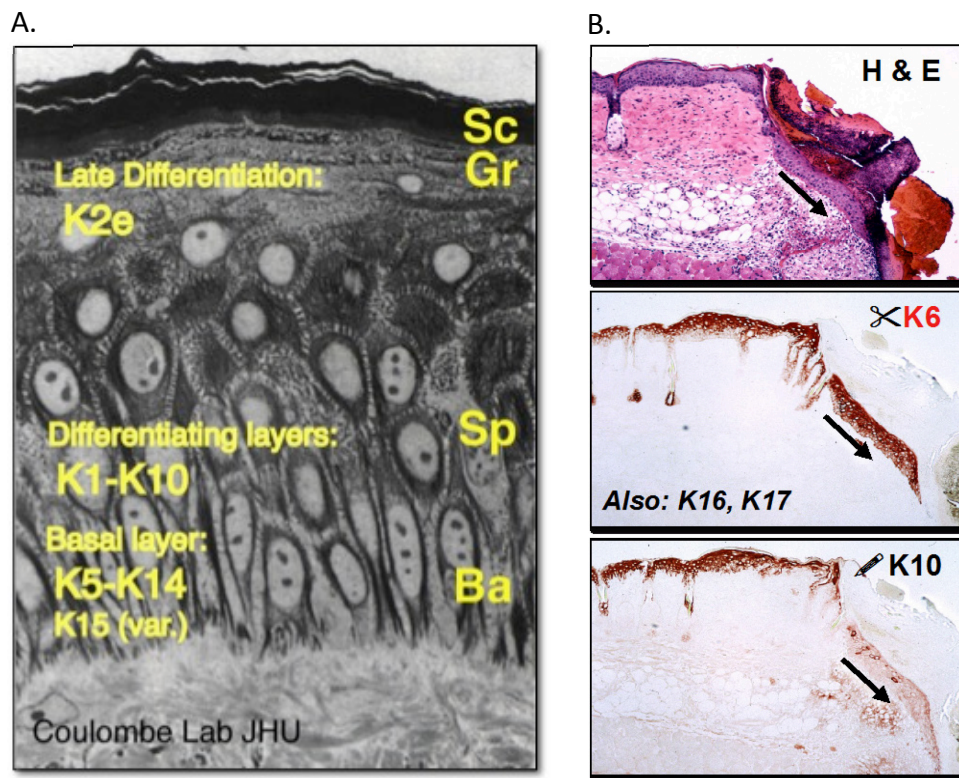


**Figure 2. Specificity of keratin expression in human epidermis.** (A) K5 and K14 are constitutively expressed in the basal layers, while K1 and K10 are constitutively expressed in the suprabasal layers of normal epidermis (adapted from Coulombe, 2011). (B) K6, K16, and K17 are robustly induced at the epidermal wound edge at the cost of keratins (ie. K10) that are normally expressed at the same site (adapted from Coulombe, 2016).

### *Pachyonychia congenita*

Pachyonychia congenita (PC) is a rare autosomal dominant genetic human skin disease that arises from mutations in keratin (*KRT*) 6a, 6b, 16, and 17 ([http://www.pachyonychia.org/pc\\_consortium.php](http://www.pachyonychia.org/pc_consortium.php)). The prevalence of PC is currently unknown, but as of 2011, approximately 1000 patients have been registered with the International PC Consortium (IPCC) ([http://www.pachyonychia.org/pc\\_consortium.php](http://www.pachyonychia.org/pc_consortium.php)). PC is characterized by painful palmoplantar keratoderma (PPK) (Figure 3), hypertrophic nail dystrophy, oral lesions, and cysts (Leachman et al., 2005). PC-associated PPK is acutely painful, debilitating, and severely compromises patient mobility (<https://ghr.nlm.nih.gov/condition/pachyonychia-congenita>). The two major subtypes of PC, PC Type 1 and PC Type 2 are caused by mutations in *KRT6a/16* and *KRT6b/17*, respectively (Smith et al., 2005). Most mutations, which can be inherited or occur de novo, are missense or small in-frame deletions located in the “hotspot” regions at the ends of the central rod domain shared by all keratins (<https://ghr.nlm.nih.gov/condition/pachyonychia-congenita>; Smith et al., 2005). Despite the molecular basis of PC having been uncovered over 20 years ago, current treatment options are limited and consist of the chemical or mechanical removal of calluses (Smith et al., 2005).



**Figure 3. Plantar skin of PC patient.** Image depicts painful PPK calluses on the soles of the feet of a PC patient with L124R K16 mutation (reproduced from IPCC gallery of PC images).

### *Keratin 16 null mice: faithful model of pachyonychia congenita-associated palmoplantar keratoderma*

Our laboratory has generated mice that are genetically null for *Krt16* (C57BL/6 strain background). *Krt16*<sup>-/-</sup> mice are born alive and are initially macroscopically indistinguishable from wild-type (*WT*) and *Krt16*<sup>+/-</sup> littermates (Lessard and Coulombe, 2012). However, the null phenotype leads to increased postnatal mortality and failure to thrive: 34% of *Krt16*<sup>-/-</sup> mice die within 24 hours after birth, compared to 6% of *WT* and 11% of *Krt16*<sup>+/-</sup> mice (Lessard and Coulombe, 2012). This can be attributed in part to defective structural integrity of the oral mucosa in *Krt16*<sup>-/-</sup> mice (Lessard and Coulombe, 2012; Lessard et al., 2013). Beginning at four weeks of age, the surviving *Krt16*<sup>-/-</sup> mice begin to exhibit striking hyperkeratotic lesions that are histologically similar to PC-associated PPK (Lessard and Coulombe, 2012). There is an upregulation of genes related to inflammation and innate immunity in the *Krt16*<sup>-/-</sup> hyperkeratotic calluses that is also consistent with PPK in individuals with PC (Lessard et al., 2013). Given the morphological and molecular similarities with PC-associated PPK, the *Krt16*<sup>-/-</sup> mouse provides the best animal model, so far, to better understand the pathogenesis of this disease.

### *Redox balance of the skin*

The skin serves a major role in defending the body against exogenous and endogenous sources of oxidative stress. Oxidative stress can arise as a consequence of defective production and/or detoxification of reactive oxygen species (ROS). In addition, harmful stimuli can evoke inflammatory responses, which if exaggerated, may aggravate pre-existing injury and cause additional tissue damage.

Glutathione (GSH) is a thiol compound essential for maintaining cellular redox balance and functions as the most abundant endogenous antioxidant (Lushchak, 2012). GSH

and glutathione disulfide (GSSG), respectively the reduced and oxidized forms of glutathione, are regulated in cycles of synthesis and regeneration (Figure 4).

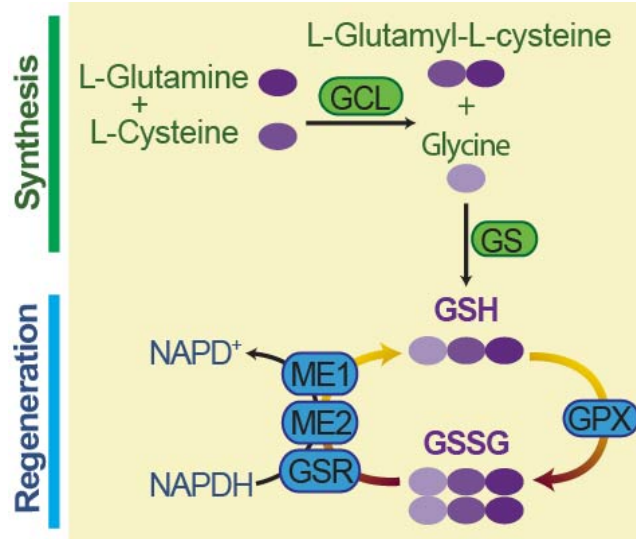


**Figure 4. Schematic representation of GSH metabolism.** GSH synthesis and regeneration are closely linked in a cycle that permits the detoxification of ROS in order to reduce cellular oxidative stress (reproduced from Kerns et al., 2016).

GSH is a tripeptide ( $\gamma$ -L-glutamyl-L-cysteinylglycine) synthesized in a two-step process through glutamate cysteine ligase (GCL) and glutathione synthetase (GS). GCL is a heterodimer that catalyzes the initial rate-determining step of GSH synthesis; it is composed of an essential catalytic subunit (GCLC) and nonessential modulatory subunit (GCLM) (Dalton et al., 2000; Yang et al., 2002). GSH can ultimately prevent oxidative damage by consuming ROS through a redox reaction that converts GSH to GSSG via glutathione peroxidase (GPX). Conversely, glutathione reductase (GSR) recycles GSSG to GSH with the simultaneous oxidation of coenzyme nicotinamide adenine dinucleotide phosphate (NADPH) (Couto et al., 2013). NADPH levels are replenished by glucose-6-phosphate dehydrogenase (G6PD) and malic enzymes 1 and 2 (ME1/2). The activities of these enzymes in GSH metabolism determine the cellular levels of GSH and GSSG and the resulting GSH/GSSG ratio (Figure 4), which is used as an important measure of cellular toxicity (Pastore et al., 2001).

### *Nrf2 signaling pathway as a regulator of redox balance*

The transcription factor nuclear factor (erythroid-derived 2)-like 2 (NRF2) is a well-known, master regulator of cellular redox homeostasis. Under basal conditions, NRF2 is sequestered in the cytoplasm by Kelch-like ECH-associating protein 1 (KEAP1) and targeted for proteasomal degradation (Itoh et al., 1999; Kobayashi et al., 2004). Oxidative and electrophilic stress results in the release, stabilization (i.e. phosphorylation), and nuclear translocation of NRF2. In the nucleus, NRF2 binds to the antioxidant responsive elements (ARE) of its target genes, which includes genes encoding antioxidants (e.g. heme oxygenase 1 (HO-1), NAD(P)H dehydrogenase quinone 1 (NQO-1)) and GSH synthesis enzymes (Figure 5; Trachootham et al., 2008; Alam and Cook, 2003; Kwak et al., 2001).

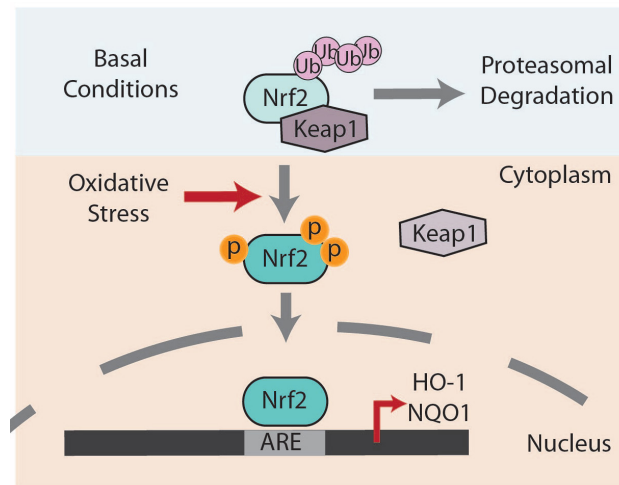


**Figure 5. Schematic representation of KEAP1-NRF2 signaling pathway.** Under basal conditions, NRF2 is sequestered by KEAP1. Upon oxidative stress, NRF2 becomes phosphorylated and enters the nucleus (adapted from Hakim, 2016).

Sulforaphane (SF) is an isothiocyanate derived from broccoli sprout extract and a pharmacological inducer of NRF2 (Zhang et al., 1992). This phytochemical has been administered to humans in both oral and topical forms (Singh et al., 2014; Dinkova-Kostova et al., 2007). Our laboratory has previously used SF as a topical treatment in the setting of a *Krt14<sup>-/-</sup>* mouse model of epidermolysis bullosa simplex (EBS), a rare genetic skin disorder caused by mutations in basal keratins K5 or K14 and characterized by trauma-induced

epithelial skin fragility and fluid-filled blisters (Coulombe et al., 2009). In this model, genetic ablation of K14 resulted in similar faulty skin integrity and blister formation, along with a postnatal mortality of approximately two-days (Kerns et al., 2007). Individuals with the equivalent of a *KRT14* null mutation have all the hallmarks of EBS, similarly to *Krt14*<sup>-/-</sup> mice (Chan et al., 1994; Rugg et al., 1994; Lloyd et al., 1995). The topical use of SF was found to induce expression of K16 and K17 to compensate for the deficiency in K14; this resulted in greatly reduced cutaneous blistering along with improved postnatal survival (Kerns et al., 2007). The rescue of the *K14*<sup>-/-</sup> phenotype displayed the powerful functional redundancy associated with keratins and offered insight into elucidating the pathophysiology and treatment options for PC.

#### *Estrogen signaling as a regulator of redox balance*

Along with NRF2 signaling, estrogen receptor (ER) signaling is also a major regulator of redox balance in humans. The two main ER isoforms, ER $\alpha$  and ER $\beta$ , are each relevant to skin biology (Table 1). In addition to its expression in classical estrogen-regulated tissues, ER $\alpha$  is stress-inducible in other tissues, including the skin, where it promotes cutaneous healing through the regulation of inflammation (Dahlman-Wright et al., 2006; Campbell et al., 2010). Conversely, ER $\beta$  is the major steroid receptor that is constitutively expressed in the skin and aids wound healing through the stimulation of re-epithelialization (Thornton et al., 2003).

	<b>ER<math>\alpha</math></b>	<b>ER<math>\beta</math></b>
Skin expression	Upregulated in times of stress	Constitutive (intrafollicular epidermis)
Role in cutaneous wound healing	Inflammation	Re-epithelialization
Impact on Nrf2 signaling	Down-regulation	Up-regulation
Regulation by estrogen	Up-regulation	Down-regulation
Mechanism of transcriptional regulation	Requires ligand binding	Majority of gene targets expressed without ligand

**Table 1. Characteristics of estrogen receptors.** ER $\alpha$  and ER $\beta$  exhibit differential and often opposing effects in the skin (adapted from Hakim, 2016).

Of particular relevance to our work are the differential effects of ER $\alpha$  and ER $\beta$  on NRF2 signaling. ER $\alpha$  is able to directly inhibit NRF2-mediated transcription via a physical interaction at the promoter region of NRF2 target genes (Ansell et al., 2005). On the other hand, activation of ER $\beta$  by the selective agonist diarylpropionitrile (DPN) promotes Nrf2 nuclear translocation through an as yet defined mechanism in human cells (Zhang et al., 2013). Moreover, high levels of ER $\beta$  may overcome ER $\alpha$ -mediated repression of NRF2 (Lo and Matthews, 2013). Taken together, these findings point to the existence of a significant yet intricate relationship between ER- and NRF2-mediated responses.

Here, we describe the utilization of the *Krt16*<sup>-/-</sup> murine model to examine the contribution of oxidative stress to the onset of PPK-like lesion in *Krt16*<sup>-/-</sup> mice and identify associated impairments in the NRF2 signaling pathway. We show that topical application of the NRF2 inducer SF prevents the formation of PPK-like lesions in male *Krt16*<sup>-/-</sup> mice. Additionally, we describe sex-specific differences in both lesion onset and SF responsiveness of *Krt16*<sup>-/-</sup> female skin that are related to fluctuations in ER $\alpha$  and ER $\beta$  expression and activation.

This thesis relates the outcome of experiments carried out by its author, alone or in collaboration with others, and is presented towards the partial fulfillment of the requirements for the Masters of Science (ScM) degree at the Johns Hopkins Bloomberg School of Public Health. The figures presented represent data directly generated by and include significant contributions from the author. The male-centric findings relevant to this thesis have been recently published in the Journal of Clinical Investigation (Kerns et al., 2016; a PDF copy of this article can be found in Appendix I), whereas the female-centric findings are being incorporated in another research manuscript currently under preparation.

## RESULTS

### *Impaired glutathione synthesis in pre-lesional male $Krt16^{-/-}$ front paw tissue*

Pre-lesional paw tissue of one-month-old  $Krt16^{-/-}$  males had a significant two-fold decrease in GSH levels relative to male  $WT$  control paw tissue, along with a net decrease in the GSH/GSSG ratio, from  $37.9 \pm 3.3$  ( $WT$ ) to  $18.5 \pm 4.7$  ( $Krt16^{-/-}$ ) (Mean  $\pm$  SEM; Appendix I, Figure 1B and C). In addition, molecular analyses revealed significant drops in GS and GCLC mRNA and protein levels, indicating that GSH synthesis enzymes were impaired, while GSR (regeneration pathway) was found to have no remarkable difference (Figure 6; Appendix I, Figure 1D and F). These findings suggest that increased oxidative stress, resulting mostly from a selective impairment of GSH synthesis, precedes the development of PPK-like lesions in  $Krt16^{-/-}$  males.

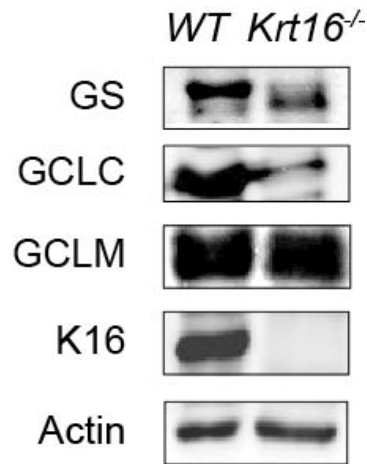


**Figure 6. Decrease in GSH synthesis in male  $Krt16^{-/-}$  pre-lesional paw skin enzymes.** Representative western blot of GSH synthesis enzymes and K16 with actin as loading control. GS, glutathione synthase; GCLC, glutamate cysteine ligase catalytic subunit; GCLM, glutamate cysteine ligase modulatory subunit (reproduced from Kerns et al., 2016).

### *Lowering GSH levels causes PPK-like alterations in $WT$ mouse skin*

To assess the impact of lowered GSH levels on paw skin morphology, we treated one-month-old  $WT$  males with intraperitoneal (i.p.) injections of 50  $\mu$ mole L-buthionine-sulfoximine (BSO), an inhibitor of GCL, twice weekly for four weeks. Relative to vehicle control, systemic BSO treatments resulted in a significant decrease of GSH ( $0.44 \pm 0.14$  fold)

and GSSG ( $0.50 \pm 0.10$  fold) in front paw tissue, while the GSH to GSSG ratio was not significantly altered (Mean  $\pm$  SEM; Figure 7A and B). Despite no noticeable macroscopic difference between experimental and control paws (Figure 7C), the BSO treatment caused a significant  $1.8 \pm 0.1$  fold increase in epidermal thickness (Mean  $\pm$  SEM; Figure 7D and E) and the appearance of PPK-like downward epidermal projections, which is reflected in an increased dermo-epidermal interface to epidermal length ratio (Figure 7F). These findings suggest that increased oxidative burden generates modest but significant PPK-like alterations in the footpad skin of *WT* mice.

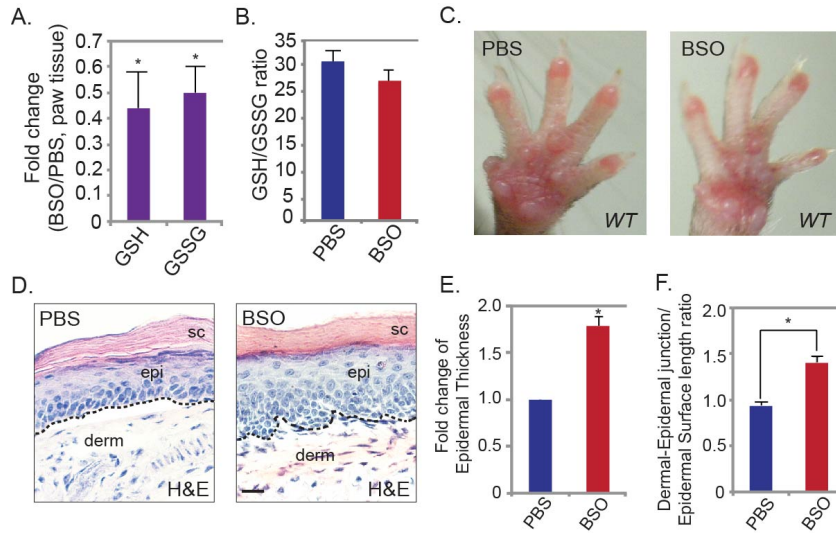


**Figure 7. Systemic BSO treatment results in increased oxidative burden and epidermal changes in male murine paw skin.** (A) Fold change of GSH and GSSG in paw tissue from 1 month old male *WT* mice treated with BSO relative to vehicle (PBS) treated controls. (B) GSH:GSSG ratio for the same mice. For A and B, data represents the mean  $\pm$  SEM of 3 biological replicates. Student's *t* test, \**P* value < 0.05. (C, D) Images and hematoxylin and eosin (H&E) staining of paw skin from 1 month old male *WT* mice treated with BSO or vehicle. Sc, stratum corneum, epi, epidermis, derm, dermis, and dotted line represents the dermo-epidermal junction. Scale bar = 50  $\mu$ m. (E) Fold change of epidermal thickness of paw skin of BSO treated mice relative to vehicle treated controls (PBS treated controls are set to one). (F) Dermo-epidermal junction/epidermal surface length ratio of paw skin of BSO and vehicle treated mice. For E and F, data calculated from 3 measurements for 2 images from 3 mice per experimental group and represents the mean  $\pm$  SEM. Student's *t* test, \**P* value < 0.05 (reproduced from Kerns et al., 2016).

*The transcription factor Nrf2 is expressed, but is hypoactive in pre-lesional male Krt16<sup>-/-</sup> front paw skin*

Since the promoter region of *KRT16* contains a functional ARE (Endo et al., 2008), we hypothesized that K16 may positively influence NRF2 activity and that this relationship may explain the impaired GSH synthesis observed in pre-lesional paws of *Krt16<sup>-/-</sup>* males (Figure 6). We found that Nrf2 and Keap1 protein levels are increased by at least two-fold in one-month-old male *Krt16<sup>-/-</sup>* paw tissue (Figure 8). The mRNA levels of *Nrf2* and *Keap1* are also increased  $13.2 \pm 2.4$  fold and  $7.7 \pm 1.7$  fold, respectively, in *Krt16<sup>-/-</sup>* male paw tissue (Mean  $\pm$  SEM; Appendix 1, Figure 2A). Since PKC $\delta$ -mediated phosphorylation of Nrf2 at serine 40 permits the release of Nrf2 from Keap1 and promotes Nrf2 stabilization and nuclear translocation (Niture et al., 2009), we assessed protein levels of phosphorylated Nrf2 (Nrf2-P, Ser40) as well as total and phosphorylated PKC $\delta$ . Protein levels of Nrf2-P were substantially decreased in *Krt16<sup>-/-</sup>* paw skin relative to control. Likewise, total PKC $\delta$  and phosphorylated PKC $\delta$  (PKC $\delta$ -P, Thr505) protein levels were also down  $2.7 \pm 0.2$  fold and  $2.9 \pm 0.3$  fold, respectively (Mean  $\pm$  SEM; Figure 8). Taken together, these findings suggest that although Nrf2 is upregulated in male *Krt16<sup>-/-</sup>* paw tissue, it is hypoactive.

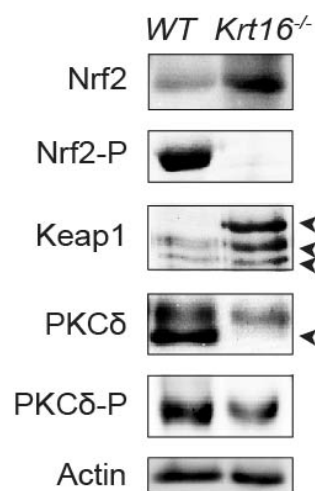


**Figure 8. Impact of *Krt16* expression on Nrf2 activation.** Representative western blot for Nrf2, Nrf2-P, Keap1, PKC $\delta$ , and PKC $\delta$ -P of three experiments with actin as loading control. Arrow heads denote the three bands of Keap1 and the lower band that represents PKC $\delta$ . Nrf2-P, phospho-Nrf2; PKC $\delta$ -P, phospho-PKC $\delta$  (reproduced from Kerns et al., 2016).

### *Elucidating the link between Krt16 and Nrf2 activation*

To examine how K16 could impact PKC $\delta$  and subsequent Nrf2 activation, we first investigated the role of receptor for activated C kinase 1 (RACK1), a scaffolding protein that has been shown to stabilize the active conformations of PKCs, including PKC $\delta$  (Adams et al., 2011). The RACK1 protein has been shown to physically interact with keratins 5 and 14, the main keratin pair of basal epidermal keratinocytes. This interaction results in sequestration of RACK1 and subsequent inhibition of PKC $\alpha$  activity upstream of desmosome assembly (Kroger et al., 2013). We hypothesized that, in contrast to K5 and K14, K16 would not interact with or sequester RACK1. In cultured 308 mouse skin keratinocytes transfected with GFP-fused K16, little to no co-localization was identified between RACK1 and K16, whereas transfected GFP-fused K14 readily co-localized with RACK1 (Appendix 1, Figure 5C). To determine the physiological consequence of the absence of physical interaction between K16 and RACK1, we also assessed RACK1 protein and mRNA levels. The *RACK1* gene is a known NRF2 target (Kim et al., 2011), so we expected to find decreased RACK1 levels in light of the Nrf2 hypoactivity observed in *Krt16*<sup>-/-</sup> skin. We measured the expression of RACK1 protein through indirect immunofluorescence and Western blotting and found that RACK1 protein was markedly reduced in pre-lesional, one-month-old male *Krt16*<sup>-/-</sup> paw skin relative to *WT* control (Figure 9A and B). The  $4.34 \pm 0.03$  fold reduction in immunofluorescence signal for RACK1 was significant ( $P < 0.01$ ) in the epidermis of *Krt16*<sup>-/-</sup> skin, relative to *WT* control (Mean  $\pm$  SEM; Appendix 1, Figure 5E). However, *RACK1* mRNA levels remained comparable between *Krt16*<sup>-/-</sup> and *WT* paw skin, suggesting faulty RACK1 protein synthesis and/or stability in the *Krt16*<sup>-/-</sup> model (Figure 9C).

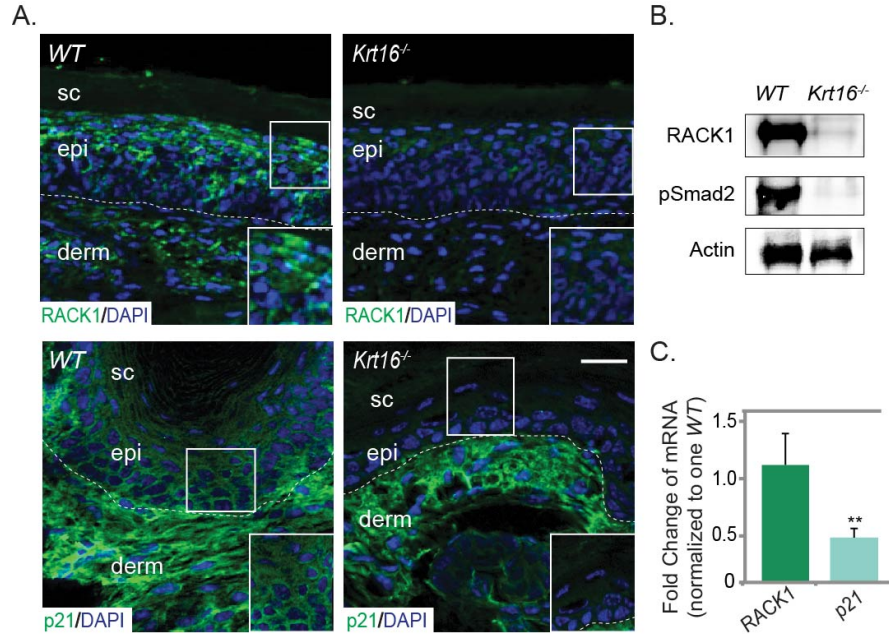


**Figure 9. A link between *Krt16* and Nrf2 activation.** (A) Indirect immunofluorescence for RACK1 and p21 in paw skin. DAPI, nuclear staining, sc, stratum corneum, epi, epidermis, derm, dermis. Dotted line marks dermo-epidermal junction. Scale bar = 50  $\mu$ m for original and 100  $\mu$ m for inset. (B) Representative western blot for RACK1 and pSmad2 of 3 experiments with actin as loading control. (C) Fold change of mRNA for *RACK1* and *p21* in pre-lesional paw skin of *Krt16*<sup>-/-</sup> mice relative to WT. Data represents the mean  $\pm$  SEM of four biological replicates. Student's t test, \*\*P value < 0.01 (reproduced from Kerns et al., 2016).

NRF2 activation in skin keratinocytes also involves the TGF- $\beta$ -dependent transcriptional activation of p21, a cyclin-dependent kinase inhibitor that competes with KEAP1 for NRF2 binding (Oshimori et al., 2015; Chen et al., 2009). *Cdkn1a*, which encodes p21, is also an established target of the TGF- $\beta$ -SMAD signaling pathway (Seoane et al., 2004; Koinuma et al., 2009). In total paw tissue, immunofluorescence signal and mRNA levels for *p21* mRNA levels were both decreased by two fold in *Krt16*<sup>-/-</sup> relative to *WT* control (Figure 9A and C). The reduction in immunofluorescence signal for p21 was significant ( $P < 0.01$ ) in *Krt16*<sup>-/-</sup> epidermis relative to *WT* control (Appendix 1, Figure 5E). Protein levels of p-SMAD2, a terminal effector of TGF- $\beta$  signaling, were also substantially lower in *Krt16*<sup>-/-</sup> compared to *WT* control (Figure 9B).

Since RACK1 has been shown to promote and be a target of TGF- $\beta$  signaling and overexpression of RACK1 has been correlated with increased p21 expression (Jia et al., 2013; Hermanto et al., 2002), we speculate that the remarkable drop in RACK1 levels in male *Krt16*<sup>-/-</sup> paw skin may contribute to lower p21 levels and impairment of TGF- $\beta$  signaling relative to WT control. Our findings indicate that K16, PKC $\delta$  activity, RACK1 protein synthesis and/or stability, TGF- $\beta$  signaling, and *p21* transcription are all intertwined in a network that can significantly modulate Nrf2 activity primarily in the suprabasal epidermis of *Krt16*<sup>-/-</sup> mice (Figure 10).

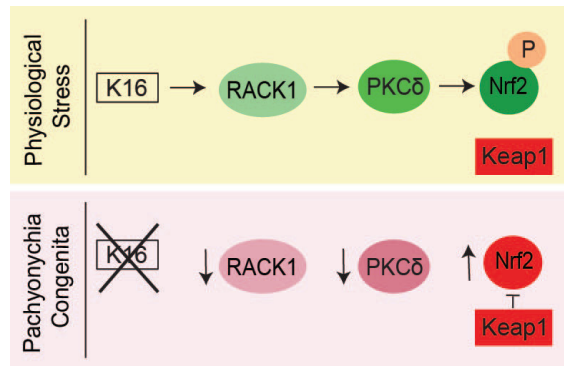
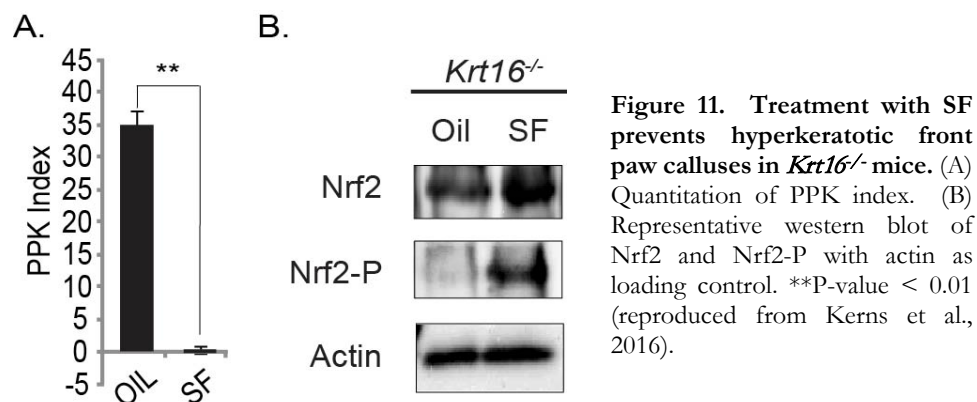


**Figure 10. Schematic of proposed regulation of Nrf2 pathway in the suprabasal epidermis under normal physiological conditions and without K16.** In the presence of K16 and under normal stress, we hypothesize that RACK1 is able to permit the PKC $\delta$ -mediated phosphorylated of NRF2. However, without in PC, this mechanism becomes aberrant (reproduced from Kerns et al., 2016).

#### *Small molecule-based activation of Nrf2 rescues PPK in male *Krt16*<sup>-/-</sup> mice*

To further investigate the role of Nrf2 hypoactivity in PPK-like lesion formation in *Krt16*<sup>-/-</sup> mice, we topically treated the front paws of one-month-old male *Krt16*<sup>-/-</sup> mice with sulforaphane (SF), an Nrf2 inducer derived from broccoli sprouts twice weekly for four consecutive weeks (Zhang et al., 1992). Macroscopically, PPK-like lesions could not be readily identified in SF-treated *Krt16*<sup>-/-</sup> males (Appendix 1, Figure 6A). A blinded assessment of the PPK index (detailed in Materials and Methods) was conducted and revealed that the average affected surface area of SF-treated paws ( $0.08 \pm 0.07$ ) was dramatically lower than those of vehicle treatment ( $34.9 \pm 3.2$ ) (Mean  $\pm$  SEM; n = 10 mice; Figure 11A).



Histological analysis showed decreased epidermal thickness following SF treatment (Appendix 1, Figure 6B). SF-treated *Krt16*<sup>-/-</sup> paws also had increased levels of Nrf2, Nrf2-P (Ser40), RACK1, PKC $\delta$ , and PKC $\delta$ -P (Figure 11B and 12; Appendix 1, Figure 6C). Interestingly, GSH levels remained similar regardless of SF or vehicle treatment, but GSSG levels decreased  $2.56 \pm 0.05$  fold after SF treatment (Mean  $\pm$  SEM; Appendix 1, Figure 6E), leading to an increase in GSH to GSSG ratio ( $19.9 \pm 0.9$  in vehicle-treated versus  $47.1 \pm 7.8$  in SF-treated *Krt16*<sup>-/-</sup> paw tissue), which indicates a decrease in oxidative stress (Mean  $\pm$  SEM; Appendix 1, Figure 6F). Surprisingly, SF treatment resulted in lower mRNA levels for both *GS* and *GCLC*, but elevated mRNA expression of *GSR* relative to vehicle oil treatment ( $6.6 \pm 2.4$  fold increase; Mean  $\pm$  SEM) (Appendix 1, Figure 6G and H). This indicates that GSH synthesis remains impaired despite Nrf2 induction, while GSH regeneration is improved. Taken together, these results suggest that topical treatment with SF successfully prevented PPK-like lesion formation, activated Nrf2, and decreased oxidative burden in one-month-old male *Krt16*<sup>-/-</sup> paw tissue.

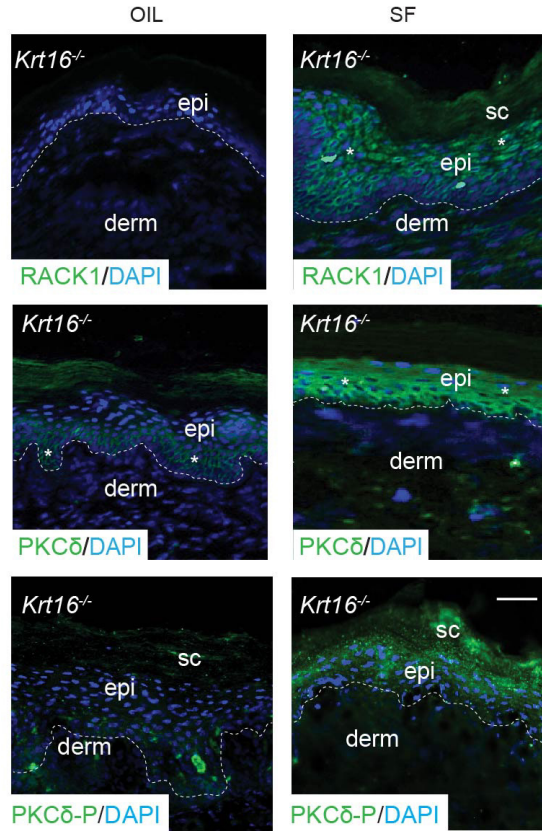


**Figure 12. Topical treatment with SF results in increase of RACK1, PKC $\delta$ , and PKC $\delta$ -P.** Representative images of indirect immunofluorescence staining for RACK1, PKC $\delta$ , PKC $\delta$ -P in *Krt16*<sup>-/-</sup> paw skin treated with SF or jojoba oil (vehicle). PKC $\delta$ -P, phospho-PKC $\delta$ ; DAPI, nuclear staining; sc, stratum corneum; epi, epidermis; derm, dermis. Scale bar = 50  $\mu$ m. Dotted line marks the dermo-epidermal junction (reproduced from Kerns et al. 2016).

#### *Topical treatment of Krt16<sup>-/-</sup> paws with SF exhibits sex-specific effects*

We postulated that the twice-weekly topical treatment regimen with SF, which successfully prevented PPK-like lesions in male *Krt16*<sup>-/-</sup> mice, would be equally effective in female *Krt16*<sup>-/-</sup> mice. Utilizing a new group of male and female *Krt16*<sup>-/-</sup> mice, we repeated the topical SF treatment regimen described above. With this second cohort of mice, we replicated our success with SF treatment in *Krt16*<sup>-/-</sup> males (Figure 13A). The PPK indices for vehicle-treated and SF-treated *Krt16*<sup>-/-</sup> male paws were  $39.1 \pm 2.4$  and 0, respectively (Mean  $\pm$  SEM; n = 8 mice per sex for each treatment group; Note: PPK = 0 indicates no lesional area noted; Figure 13B). Surprisingly, SF treatment did not appear to impact lesion development in female *Krt16*<sup>-/-</sup> mice (Figure 13A). There was no significant difference between the PPK indices for vehicle-treated and SF-treated female *Krt16*<sup>-/-</sup> paws ( $11.9 \pm 2.6$  versus  $10.1 \pm 0.6$ , respectively;

Mean  $\pm$  SEM; n = 8 mice per sex for each treatment group). Unlike the *Krt16*<sup>-/-</sup> males, the *Krt16*<sup>-/-</sup> females showed no reduction of epidermal thickening of paw skin following SF treatment (Figure 13C).

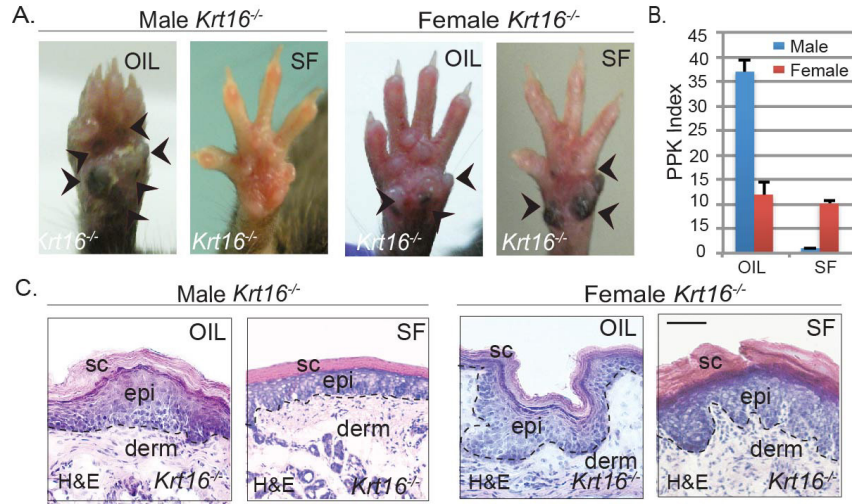


**Figure 13. Topical treatment of *Krt16*<sup>-/-</sup> paws with SF has sex-specific effects.** (A) Representative images of male and female *Krt16*<sup>-/-</sup> paws following SF or vehicle (OIL) treatment. Arrow heads point to affected areas. PPK index following SF or vehicle (OIL) treatment per sex. Mean  $\pm$  SEM. n = 8 mice per sex. (C) H&E staining of male and female *Krt16*<sup>-/-</sup> paws following SF or vehicle (OIL) treatment. Scale bar = 50  $\mu$ m (adapted from Kerns et al., unpublished data).

#### *Manipulation of ER signaling impacts responsiveness to SF treatment in female *Krt16*<sup>-/-</sup> mice*

Given the opposing effects of ER $\alpha$  and ER $\beta$  on each other and on Nrf2 signaling, and their fluctuating levels in female *Krt16*<sup>-/-</sup> paw tissue (Kerns et al., unpublished data), we postulated that a dominance of ER $\alpha$  over ER $\beta$ , may explain the failure of SF treatments to activate NRF2 in female *Krt16*<sup>-/-</sup> paw tissue. We developed a combination treatment consisting of i.p. injections of 5 $\mu$ g/kg mouse DPN in addition to topical SF for treating one-month-old *Krt16*<sup>-/-</sup> females. After treating twice weekly for four weeks, front paws were harvested for morphological analysis and indirect immunofluorescence. *Krt16*<sup>-/-</sup> females that received both DPN and SF had a remarkable absence of PPK-like lesions on front paws relative to SF-

treated controls (Figure 14A). Indirect immunofluorescence staining for NRF2 and p-NRF2 indicated a mild increase in total NRF2 protein, but a striking activation of NRF2 in the basal cell layer of the epidermis as well as an increase of NQO-1 in dual treated *Krt16*<sup>-/-</sup> females (Figure 14B). These findings indicate that SF responsiveness in *Krt16*<sup>-/-</sup> females may be influenced by ER signaling. Indirect immunofluorescence staining for these targets in an additional control group treated only with DPN are currently in progress.

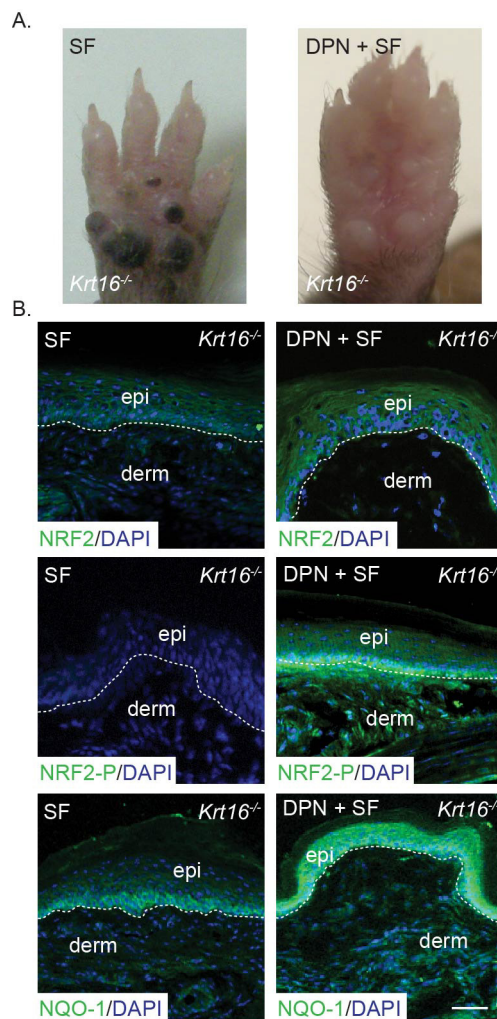


**Figure 14. Manipulation of ER signaling impacts responsiveness to SF treatment in *Krt16*<sup>-/-</sup> female mice.** (A) Representative images of *Krt16*<sup>-/-</sup> female paws following DPN and SF or SF-only treatment. (B) Representative images of indirect immunofluorescence staining for NRF2, NRF2-P, and NQO-1 in *Krt16*<sup>-/-</sup> female paw skin treated with DPN and SF or SF-only treatment. NRF2-P, phospho-NRF2; DAPI, nuclear staining; epi, epidermis; derm, dermis. Scale bar = 50  $\mu$ m. Dotted line marks the dermo-epidermal junction (adapted from Kerns et al., unpublished data).

## DISCUSSION

In this thesis, we determined that oxidative stress associated with decreased GSH synthesis and misregulated NRF2 signaling precedes the formation of PPK-like lesions in male *Krt16*<sup>-/-</sup> mice. We linked the NRF2 hypoactivity observed in *Krt16*<sup>-/-</sup> paw skin to the hypoactivity of its upstream modifiers, RACK1 and PKC $\delta$ . Moreover, we find that topical treatment with an NRF2 inducer, SF, prevents these PPK-like lesions and restores redox balance. Finally, we uncover a sex bias in how Nrf2 is regulated in skin keratinocytes of male vs. female skin keratinocytes.

Taken together, these findings pinpoint a potential role for K16 in the regulation of the oxidative stress response of the skin, possibly through the modulation of NRF2 signaling. Upon wounding or stress to the skin epithelium, both K16 and NRF2 are upregulated in epidermal keratinocytes (Paladini et al., 1996; Braun et al., 2002). Our laboratory previously found that *Krt16* expression is typically confined to the suprabasal epidermis (Paladini et al., 1996). In response to ultraviolet (UV) B irradiation, Nrf2 is known to stimulate GSH synthesis and distribution in suprabasal keratinocytes and subsequently protect neighboring basal cells via a GSH-mediated gradient (Schafer et al., 2010). Our study demonstrates that the loss of *Krt16* specifically affects Nrf2-regulated GSH production. We find that K16 does not appear to sequester RACK1, in contrast to K5 and K14, and that the lack of K16 also results in lower RACK1 protein levels and phosphorylated PKC $\delta$  in hairless skin. In addition, TGF- $\beta$  signaling through SMAD2 and TGF- $\beta$  activation of p21, an NRF2 stabilizer, are impaired without the presence of K16. K16 expression is known to be stimulated by TGF- $\beta$  (Choi and Fuchs, 1990), thus our findings suggest that K16 may influence redox balance in glabrous skin keratinocytes through an intricate signaling web involving NRF2, PKC $\delta$ , RACK1, p21, and

TGF- $\beta$ . The effect of K16 on TGF- $\beta$  signaling may lend support to a previously deduced epidermal gradient of NRF2 that results from UVB irradiation-induced stress (Schafer et al., 2010). Taken together, we suggest that K16 may be a major player in maintaining redox balance in the epidermis of glabrous skin and that K16 may control NRF2 activation in skin keratinocytes experiencing stress.

Another key finding from our study has been the ineffectiveness of SF in female *Krt16*<sup>-/-</sup> mice, which may be related to ER signaling. The phenotypic rescue in male *Krt16*<sup>-/-</sup> mice establishes the importance of the NRF2 pathway in the pathophysiology of PPK-like lesions. However, SF treatment alone was not sufficient to prevent lesion formation in female *Krt16*<sup>-/-</sup> mice. In a revised treatment regimen for *Krt16*<sup>-/-</sup> females, we were able to inhibit PPK-like lesion formation by supplementing SF treatments with ER $\beta$  agonist, DPN. Given that ER $\beta$  has been shown to promote Nrf2 nuclear translocation (Zhang et al., 2013), these results suggest that estrogen receptor signaling could be a notable player in lesion formation and SF responsiveness.

Whether oxidative stress stemming from alterations in GSH production and/or metabolism plays a similar role in the pathophysiology of PPK in PC patients remains to be investigated. Despite uncovering the molecular basis of PC as a keratin gene disorder over 20 years ago, current treatment options (e.g. mechanical or surgical removal of calluses, allele-specific silencing) are limited and ineffective (Smith et al., 2005). The pharmacological restoration of redox balance and NRF2 signaling represents an additional, and potentially more effective, avenue through which to achieve a substantial clinical improvement of PPK. Our enriched understanding of the pathophysiology of PC-associated PPK sheds insight into mechanisms behind conditions of impaired wound healing or oxidative stress response and therapeutic pathways through which to treat them.

## MATERIALS AND METHODS

### *Animals, antibodies, and preparation of SF and DPN treatments*

A *Krt16*<sup>-/-</sup> mouse line (C57BL/6 strain background) were generated by our laboratory and has since been maintained under specific pathogen-free conditions (Lessard et al., JID, 2012). Commercial antibodies used include  $\beta$ -actin (sc-47778, Santa Cruz), GCLC (sc-28965, Santa Cruz), GCLM (ab124827, Abcam), GS (ab91591, Abcam), Keap1 (#4617S, Cell Signaling), Nrf2 (sc-13032, Santa Cruz), p-Nrf2 (PAR2020, NeoBiolab), PKC $\delta$  (sc-213, Santa Cruz), p-PKC $\delta$  (#9374, Cell Signaling), RACK1 (sc-17754, Santa Cruz), and p-Smad2 (#3101, Cell Signaling). Generation of the anti-K16 antibody has been previously described (Bernot et al., JID, 2002). Alexa Fluor-conjugated and HRP-conjugated secondary antibodies (Life Technologies) were also used for indirect immunofluorescence and Western blotting, respectively. Sulforaphane (SF) was obtained from LKT Laboratories and jojoba oil (vehicle) was obtained from MP Biomedicals LLC. Stock solutions of SF were maintained at 0.1M in DMSO and diluted to the desired final concentration in jojoba oil for topical application on the day of the treatment (Kerns et al., Mol Cell Biol, 2010; Dinkova-Kostova et al., Cancer Epidemiol Biomarkers Prev, 2007). DPN was obtained from Sigma-Aldrich and 1X PBS (vehicle) was obtained from Life Technologies. Stock solutions of DPN were maintained at 1 $\mu$ M in DMSO and diluted to the desired final concentration in PBS for i.p. injection on the day of the treatment (Campbell et al., JEM, 2010).

### *Mouse studies*

All studies involving mice were reviewed and approved by the Johns Hopkins University Institutional Animal Care and Use Committee.

Four- and six-week-old *Krt16*<sup>-/-</sup> or WT male mice were topically treated with either 100µl of 1µmole SF or vehicle control on their front paws twice weekly for four weeks, after which the front paws were harvested for biochemical and morphological analysis. The ventral surface of each treated paw was photographed and the extent of PPK-like lesions was blindly and independently assessed by five individuals.

Four-week-old WT mice were given i.p. injections of 50µmole BSO (Sigma-Aldrich), an inhibitor of GSH synthesis, in PBS or PBS alone twice weekly for four weeks (Kerns et al., Mol Cell Biol, 2010). Upon completion of treatment, the front paws were harvested for molecular and histological analysis.

Four-week-old *Krt16*<sup>-/-</sup> or WT female mice were topically treated in the same manner as the male counterparts and received i.p. injections of 5µg/kg mouse DPN, an ERβ agonist, in PBS or PBS alone twice weekly for four weeks. Post-treatment harvest and analysis were performed identically to the male counterparts.

#### *Biochemical and morphological analysis*

The PPK index was generated from a blinded assessment of 10-15 front paw images de-identified for age, sex, genotype, and type of treatment received. Each paw was evaluated for percentage of area affected by hyperpigmentation at 10 different pressure sites. Each set of PPK indices was assessed by 3-5 individuals, all of whom had no involvement in the compilation of images. RNA was extracted from front paws using TriPure Isolation Reagent (Sigma-Aldrich) and purified with DNase treatment using NucleoSpin RNA Clean-up (Macherey-Nagel). The amount of 1µg of total RNA from each sample was reverse transcribed using an iScript cDNA Synthesis Kit (Bio-Rad) and quantitative RT-PCR was performed as described (Hobbs et al., Nat Genet, 2015). Target-specific oligonucleotide primer sets were

used and are listed in Table 2. Protein was also extracted from front paws using TriPure Isolation Reagent (Sigma-Aldrich) and concentration was measured using a Bradford Assay Kit (Bio-Rad). For Western blotting, protein (15-20 $\mu$ g) was loaded onto 10% SDS-PAGE gels and blotted onto nitrocellulose membranes using standard methods. Blocking conditions, as well as primary and secondary antibody dilution buffers, used 5% BSA (P212121 store). Actin was used as a loading control in all immunoblots. Bound primary antibodies were detected with enhanced chemiluminescence (Therm Scientific) and imaged using the FluorChem Q system. GSH and GSSG levels in paw tissue were assessed using the Glutathione Fluorometric Assay Kit (BioVision). For histological analysis, paw tissue was embedded in OCT (Sakura Finetek), frozen in dry ice, and stored at -20°C upon sectioning. Tissue sections were consistently cut at 8 $\mu$ m in a transverse orientation relative to paw morphology. Histopathology was obtained through H&E staining and indirect immunofluorescence was performed with primary and Alexa Fluor-conjugated secondary antibodies (Hobbs et al., Nat Genet, 2015).

### *Statistics*

Unpaired 2-tailed Student's *t* test and ANOVA were performed for statistical analysis. Significant differences between two groups are noted by individual or paired asterisks in the figures included in this thesis. Blinded quantitation of indirect immunofluorescence and Western blotting was performed using ImageJ (NIH) and relevant data is presorted as mean  $\pm$  SEM (Standard Error of the Mean).

**Table 2.** List of oligonucleotide primer sequences.

Target	Forward	Reverse
<i>Actin</i>	5'-TGGAATCCTGTGGCATCCATGAAAC-3'	3'-TAAAACGCAGCTCAGTAACAGTCCG-5'
<i>G6PD</i>	5'-ACCATCTGGTGGCTGTTCC-3'	3'-CATTCATGTGGCTGTTGAAGG-5'
<i>Gclb</i>	5'-ACATCTACCACGCAGTCAAGGACC-3'	3'-CTCAAGAACATCGCCTCCATTTCAG-5'
<i>Gclm</i>	5'-GCCCCGCTCGCCATCTCTC-3'	3'-GTTGAGCAGGTTCCCGGTCT-5'
<i>Gs</i>	5'-CAAAGCAGGCCATAGACAGGG-3'	3'-AAAAGCGTGAATGGGGCATAC-5'
<i>Hmox1</i>	5'-CTGTGTAACCTCTGCTGTTCC-3'	3'-CCACACTACCTGAGTCTACC-5'
<i>Keap1</i>	5'-CATCCACCCTAAGGTCATGGA-3'	3'-GACAGGTTGAAGAACTCCTCC-5'
<i>Me1</i>	5'-GATGATAAGGTCTTCCTCACC-3'	3'-TTACTGGTTGACTTTGGTCTGT-5'
<i>Me2</i>	5'-TTCTTAGAAGCTGCAAAGGC-3'	3'-TCAGTGGGGAAGCTTCTCTT-5'
<i>Nqo1</i>	5'-AGGATGGGAGGTACTCGAATC-3'	3'-AGGCGTCCTTCCTTATATGCTA-5'
<i>Nrf2</i>	5'-TCTCCTCGCTGGAAAAAGAA-3'	3'-AATGTGCTGGCTGTGCTTTA-5'
<i>p21</i>	5'-CGAGAACGGTGGAACTTTGAC-3'	3'-CAGGGCTCAGGTAGACCTTG-5'
<i>Rack1</i>	5'-AGGGCCACAATGGATGGGTA-3'	3'-CAGCTTCCACATGATGATGGTC-5'

# APPENDIX I

Downloaded from <http://www.jci.org> on August 16, 2016. <http://dx.doi.org/10.1172/JCI84870>

RESEARCH ARTICLE

The Journal of Clinical Investigation

## Oxidative stress and dysfunctional NRF2 underlie pachyonychia congenita phenotypes

Michelle L. Kerns,<sup>1</sup> Jill M.C. Hakim,<sup>1</sup> Rosemary G. Lu,<sup>1</sup> Yajuan Guo,<sup>1</sup> Andreas Berroth,<sup>2</sup> Roger L. Kaspar,<sup>3</sup> and Pierre A. Coulombe<sup>4,5,6</sup>

<sup>1</sup>Department of Biochemistry and Molecular Biology, Bloomberg School of Public Health, Johns Hopkins University, Baltimore, Maryland, USA, <sup>2</sup>Department of Pediatrics, Stanford University School of Medicine, Stanford, California, USA, <sup>3</sup>TransDerm Inc., Santa Cruz, California, USA, <sup>4</sup>Department of Biological Chemistry, <sup>5</sup>Department of Dermatology, and <sup>6</sup>Department of Oncology, School of Medicine, Johns Hopkins University, Baltimore, Maryland, USA.

Palmoplantar keratoderma (PPK) are debilitating lesions that arise in individuals with pachyonychia congenita (PC) and feature upregulation of danger-associated molecular patterns and skin barrier regulators. The defining features of PC-associated PPK are reproduced in mice null for keratin 16 (*Krt16*), which is commonly mutated in PC patients. Here, we have shown that PPK onset is preceded by oxidative stress in footpad skin of *Krt16*<sup>-/-</sup> mice and correlates with an inability of keratinocytes to sustain nuclear factor erythroid-derived 2 related factor 2-dependent (NRF2-dependent) synthesis of the cellular antioxidant glutathione (GSH). Additionally, examination of plantar skin biopsies from individuals with PC confirmed the presence of high levels of hypophosphorylated NRF2 in lesional tissue. In *Krt16*<sup>-/-</sup> mice, genetic ablation of *Nrf2* worsened spontaneous skin lesions and accelerated PPK development in footpad skin. Hypoactivity of NRF2 in *Krt16*<sup>-/-</sup> footpad skin correlated with decreased levels or activity of upstream NRF2 activators, including PKC $\delta$ , receptor for activated C kinase 1 (RACK1), and p21. Topical application of the NRF2 activator sulforaphane to the footpad of *Krt16*<sup>-/-</sup> mice prevented the development of PPK and normalized redox balance via regeneration of GSH from existing cellular pools. Together, these findings point to oxidative stress and dysfunctional NRF2 as contributors to PPK pathogenesis, identify K16 as a regulator of NRF2 activation, and suggest that pharmacological activation of NRF2 should be further explored for PC treatment.

### Introduction

Since the genetic etiology of the bullous skin disease epidermolysis bullosa simplex was uncovered in 1991 (1), more than 100 distinct disorders have been shown to arise from or be promoted by mutations in an intermediate filament (IF) gene (2, 3). In most instances, these disorders are rare and caused by dominantly acting small mutations that affect the coding sequence of the target IF gene or, more rarely, the splicing of its precursor mRNA. Reflecting the exquisitely tissue-specific and context-dependent regulation of most individual IF genes, these disorders clinically manifest in a very distinctive and typically restricted fashion (4, 5). Whereas the pathophysiology underlying IF-based disorders ranges from the relatively simple (e.g., cell/tissue fragility) to the very complex (e.g., premature aging), the development of effective treatments has been lagging owing to a variety of factors including, in part, the plurality of mutations associated with any individual disorder and IF gene (4, 6).

Pachyonychia congenita (PC) is a rare condition typified by marked nail dystrophy, palmoplantar keratoderma (PPK), oral lesions, and cystic skin lesions (7). PC is caused by mutations affecting either the type II keratin paralogs *KRT6A*, *KRT6B*, or *KRT6C* or the related type I keratin *KRT16* or *KRT17* genes (7, 8). Consistent with the clinical presentation of PC, these keratin genes are normally expressed in ectoderm-derived epithelial appendages and

in the thicker epidermis of palms and soles, but not in interfollicular epidermis (9). Whereas one observes a pronounced degree of variation in the severity of clinical features across individuals, PPK clearly constitutes the most debilitating aspect of PC and, given the associated pain, has a pronounced if not devastating impact on ambulation and quality of life (7, 10). The pathophysiology of PC is in fact quite complex and has perplexed clinicians and biologists alike for years. In part, this likely reflects the fact that K6a, K6b, K16, and K17 have distinct properties and functions among keratins (5). Further, *Krt6a*, *Krt6b*, *Krt16*, and *Krt17* are highly inducible upon disruption of homeostasis in most complex epithelia (9, 11), and this property likely adds to the chronic and progressively worsening character of PPK lesions in individuals with PC (12). The poor understanding of the pathophysiology of PPK and PC has unfortunately contributed to delays in devising effective treatments in spite of a well-organized patient- and researcher-based effort to combat this disease, as exemplified in the International Pachyonychia Congenita Consortium (IPCC).

Mice homozygous for a null allele at the *Krt16* locus develop a PC-like presentation that includes, in those animals surviving perinatal lethality, the development of spectacular PPK lesions in a completely penetrant fashion by 6 weeks of age (13). Calluses arise preferentially at sites of mechanical pressure in the footpads of *Krt16*<sup>-/-</sup> mice and otherwise feature all of the hallmarks of PC-related PPK, including modest hyperproliferation along with massive thickening of the living epithelium and stratum corneum layers of the epidermis (referred to as hyperkeratosis) (7, 13). Interestingly, established PPK lesions in *Krt16*<sup>-/-</sup> mice show little evidence of cell

**Authorship note:** J.M.C. Hakim and R.G. Lu contributed equally to this work.  
**Conflict of interest:** The authors have declared that no conflict of interest exists.  
**Submitted:** September 29, 2015; **Accepted:** March 24, 2016.  
**Reference information:** *J Clin Invest*. 2016;126(6):2356–2366. doi:10.1172/JCI84870.

JCI

2356

jci.org Volume 126 Number 6 June 2016

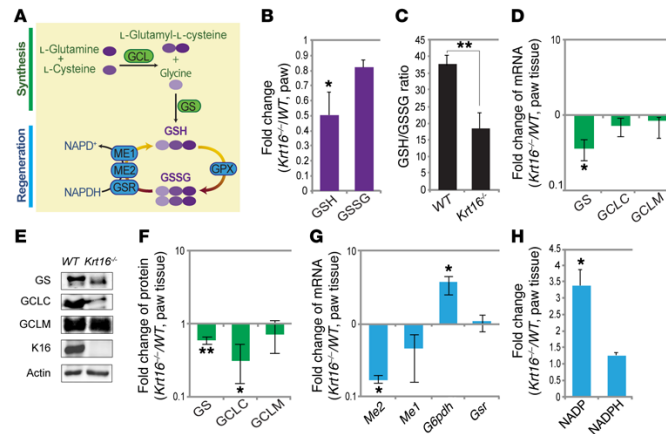


**Figure 1. Decrease in GSH synthesis in *Krt16*<sup>-/-</sup> prelesional paw skin.** (A) Schematic representation of GSH synthesis and metabolism. (B) Fold change in GSH and GSSG for *Krt16*<sup>-/-</sup> relative to WT. (C) GSH to GSSG ratio for *Krt16*<sup>-/-</sup> and WT paw skin. For B and C, data represent mean  $\pm$  SEM of 6 biological replicates. Student's *t* test. (D) Relative fold change in mRNA levels of GSH synthesis enzymes. Data represent mean  $\pm$  SEM of 4 to 6 biological replicates. Student's *t* test. (E) Representative Western blot of GSH synthesis enzymes and K16 with actin as loading control. (F) Histogram of quantitation of Western blot data. Data represent mean  $\pm$  SEM of 3 biological replicates and are normalized to actin. Student's *t* test. (G) Relative fold change in mRNA levels of GSH metabolism enzymes. Data represent mean  $\pm$  SEM of 4 to 6 biological replicates. Student's *t* test. For D, F, and G, log scale. (H) Relative fold change of total NADP and NADPH. Data represent mean  $\pm$  SEM of 6 biological replicates involving 1-month-old male mice. Student's *t* test. \**P* < 0.05; \*\**P* < 0.01.

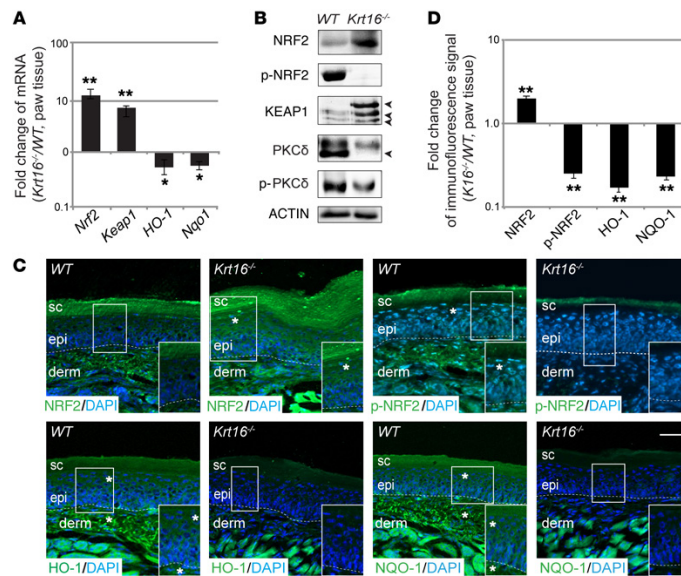
fragility (11). A follow-up effort showed that footpad lesions from *Krt16*<sup>-/-</sup> mouse paw skin and biopsies from clinically involved planar skin in individuals with PC show a remarkably similar molecular signature whereby the expression of genes coding for danger-associated molecular patterns (DAMPs), e.g., alarmins, and regulators of skin barrier formation, is markedly elevated (11). This effort also showed that subjecting clinically uninvolved skin in *Krt16*<sup>-/-</sup> mice to wounding or topically applied chemical irritants results in an exaggerated upregulation of DAMP/alarmin and skin barrier genes relative to controls and, further, that *Krt16* is an integral part of a strong genetic network involving such genes (11). Here, we provide compelling evidence that K16 regulates the function of nuclear factor erythroid-derived 2 related factor 2 (NRF2), a master regulator of cellular responses to oxidative stress and of epidermal homeostasis, suggesting a new avenue for the therapeutic management of PC-associated PPK lesions.

## Results

**Impaired glutathione synthesis in prelesional *Krt16*<sup>-/-</sup> front paw tissue.** Glutathione (GSH) is the most abundant endogenous antioxidant in cells and is crucial for the maintenance of cellular redox balance (14). GSH prevents damage from ROS in part by consuming ROS through a reduction reaction that converts reduced GSH to its oxidized state (glutathione disulfide [GSSG]). The ratio of GSH to GSSG is routinely used as a measure of cellular toxicity (15). GSH is a tripeptide ( $\gamma$ -L-glutamyl-L-cysteinylglycine) synthesized through a 2-step process catalyzed by the enzymes glutamine cysteine ligase (GCL) and glutathione synthetase (GS). GCL is a heterodi-

mer that catalyzes the initial rate-limiting step of GSH synthesis and is composed of an essential catalytic subunit (GCLC) (16) and a modulatory subunit (GCLM) that enhances the efficiency of GCL, but is not required for function (17). GSH can also be regenerated from GSSG in a reaction that is catalyzed by the enzyme glutathione reductase (GSR) and utilizes the coenzyme NADPH as an electron donor (18). In turn, levels of NADPH are replenished by the action of glucose-6-phosphate dehydrogenase (G6PD) and malic enzymes 1 and 2 (ME1/2). The levels and activities of each of these enzymes (see Figure 1A) contribute to set the cellular levels of GSH and GSSG and the resulting GSH/GSSG ratio.

We previously reported that pharmacological manipulation of GSH levels upregulates *Krt16* expression in murine epidermis (19). Here, we set out to characterize the redox balance in prelesional paw skin of 1-month-old male *Krt16*<sup>-/-</sup> mice. Relative to control, *Krt16*<sup>-/-</sup> paw tissue had a significant 2-fold decrease in GSH levels and slightly reduced GSSG levels (Figure 1B). The net effect was a lower GSH to GSSG ratio ( $18.5 \pm 4.7$  for *Krt16*<sup>-/-</sup> paws versus  $37.9 \pm 3.3$  for WT control), indicative of more oxidative stress in *Krt16*<sup>-/-</sup> skin relative to WT skin (Figure 1C). To test whether the decline in GSH in *Krt16*<sup>-/-</sup> paw skin was due to alterations in de novo synthesis or regeneration, we assessed the expression of relevant enzymes. There was a notable  $2.8 \pm 0.1$ -fold drop in GS mRNA (Figure 1D; mean  $\pm$  SEM) and markedly less GS and GCLC protein relative to control (Figure 1, E and F). In contrast, we found no remarkable difference in *Gsr* mRNA (Figure 1G). Although the mRNA levels of *Me2* and *G6pd* were decreased  $5.3 \pm 0.2$ -fold and increased  $3.7 \pm 0.9$ -fold, respectively, the overall levels of NADPH were similar



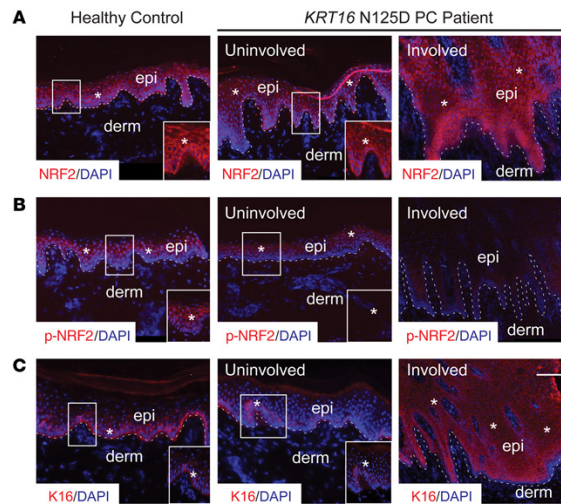
to those of control (Figure 1H; mean  $\pm$  SEM). Taken together, these findings suggest that GSH synthesis is impaired in murine paw tissue lacking *Krt16*, creating a state of oxidative stress prior to the onset of hyperkeratotic lesions.

**Lowering GSH levels causes PPK-like alterations in WT mouse skin.** To gauge the effect of enhanced oxidative stress alone on skin morphology, we next treated 1-month-old WT male mice through i.p. injections of 50  $\mu$ mol/L 1-buthionine-sulfoximine (BSO), an inhibitor of GSH synthesis, twice weekly. Levels of GSH and GSSG in paw tissue were assessed, and histological analysis was performed after 4 weeks of treatment. Relative to vehicle control, systemic BSO resulted in a significant decrease of both GSH and GSSG in paw tissue (Supplemental Figure 1A; supplemental material available online with this article; doi:10.1172/JCI84870DS1). The ratio of GSH to GSSG remained within normal limits (Supplemental Figure 1B). Although BSO treatment did not cause any obvious macroscopic changes of the paws (Supplemental Figure 2C), it resulted in a significant,  $1.8 \pm 0.1$ -fold, increase of epidermal thickness (Supplemental Figure 1, D and E; mean  $\pm$  SEM) along with the appearance of marked, PPK-like downward epidermal projections, which is quantitatively reflected through a measurement of the relative length of the dermoepi-

dermal interface (Supplemental Figure 1, D and F). These findings establish that even a time-limited state of oxidative burden suffices to induce epidermal changes related to PPK lesions and lend strong support for their potentially important influence upon the pathogenesis of PC-related PPK.

**The transcription factor NRF2 is expressed but hypoactive in lesioned *Krt16*<sup>-/-</sup> footpad skin.** NRF2 regulates a transcriptional program that preserves cellular redox homeostasis and includes a myriad of GSH synthesis and metabolism genes. NRF2 acts through antioxidant response elements (AREs) that are located in the promoter regions of these genes (20). The promoter region of *Krt16* contains a functional ARE (21). We hypothesized that K16 may itself contribute to NRF2 activity in the setting of a positive feedback loop and that the defect in GSH synthesis observed in *Krt16*<sup>-/-</sup> paw tissue reflects a malfunctioning of the NRF2 signaling pathway.

We first evaluated the status of NRF2/KEAP1 signaling ahead of the development of PPK-like lesions in footpad skin of *Krt16*<sup>-/-</sup> mice. Surprisingly, loss of *Krt16* caused a  $13.2 \pm 2.4$ -fold increase of *Nrf2* mRNA as well as a 2-fold increase in NRF2 protein in paw tissue of 1-month-old *Krt16*<sup>-/-</sup> male mice (Figure 2, A–D; mean  $\pm$  SEM). In striking contrast, the mRNA levels of 2 classical NRF2 target genes, heme oxygenase 1 (*HO-1*) and NAD(P)H dehydroge-



nase quinone 1 (*Nqo1*) (22, 23), were approximately 2-fold lower in *Krt16*<sup>-/-</sup> relative to control paw skin (Figure 2A). This corresponded with  $5.9 \pm 0.2$ -fold and  $6.7 \pm 0.4$ -fold decreases in the immunofluorescence signal for HO-1 and NQO-1 in *Krt16*<sup>-/-</sup> epidermis relative to control (Figure 2, C and D). Taken together with the marked reduction in GSH synthesis (Figure 1), these findings imply that, although NRF2 transcript and protein levels are increased, there is an impairment of the NRF2 signaling pathway in 1-month-old *Krt16*<sup>-/-</sup> paw skin, prior to the development of PPK lesions.

We assessed whether the loss of K16 could be impeding NRF2 activation through KEAP1, the cytoplasmic inhibitor that normally binds to NRF2 and promotes its proteosomal degradation (24). *Keap1* mRNA levels were  $7.7 \pm 1.7$ -fold higher in *Krt16*<sup>-/-</sup> paw skin (Figure 2A), and the levels of KEAP1 protein were also elevated approximately 2-fold (Figure 2B). This said, the occurrence of high levels of NRF2 protein imply that the reduction of NRF2 activity is unlikely solely due to altered function of KEAP1 in the absence of K16.

PKC $\delta$ -mediated phosphorylation of NRF2 at serine 40 is required for release of NRF2 from KEAP1 and its subsequent stabilization and nuclear translocation (25), affording an additional opportunity to assess NRF2 activity status. Phosphorylated NRF2 (p-NRF2) (Ser40) was decreased in *Krt16*<sup>-/-</sup> skin, as detected by both Western blotting (Figure 2B) and indirect immunofluorescence (Figure 2, C and D). Protein levels of total PKC $\delta$  and PKC $\delta$  phosphorylated at Thr505, which is located in the activation loop, were also reduced in *Krt16*<sup>-/-</sup> paw tissue relative to control (Figure 2D). Total PKC $\delta$  and p-PKC $\delta$  (Thr505) levels were down  $2.7 \pm 0.2$ -fold and  $2.9 \pm 0.3$ -fold, respectively, in *Krt16*<sup>-/-</sup> paw

tissue relative to control (mean  $\pm$  SEM;  $n = 3$ ). Together, these findings establish that the transcription factor NRF2 is present in abundance, but dysfunctional in prelesional footpad skin of *Krt16*<sup>-/-</sup> mice, correlating with impaired expression and activity of its upstream regulator PKC $\delta$ .

*NRF2 is present but hypoactive in lesional plantar epidermis of individuals with PC.* To test the clinical applicability of our findings in the *Krt16*<sup>-/-</sup> mouse model, we evaluated NRF2 and p-NRF2 expression in plantar skin of individuals suffering from PC. Genetically, the PC samples surveyed included a *KRT16*N125D mutation (Figure 3), a *KRT6c*N172D mutation (Supplemental Figure 2), a *KRT6a*D432\_E470dup mutation (data not shown), and a *KRT6a* N172del mutation (data not shown).

In all 4 PC cases as well as the plantar skin of a healthy volunteer, substantial expression of NRF2 can be detected in plantar epidermis via indirect immunofluorescence, irrespective of the presence of lesions. By contrast, expression of p-NRF2 is markedly lower in the lesional epidermis of individuals with PC when compared with clinically normal-appearing skin from a proximal area in the same individual's plantar skin (e.g., compare "involved" and "uninvolved" in Figure 3B) and in plantar epidermis from a healthy volunteer (Figure 3B; see also Supplemental Figure 2). Consistent with a previous study (8), expression of K16 was also increased in lesional skin tissue from the individual with *KRT16*N125D PC relative to plantar skin of a healthy volunteer (Figure 3C). These observations corroborate the findings in the *Krt16*<sup>-/-</sup> mouse model and support a possible association between PPK lesions and hypoactive NRF2. They further suggest that impaired NRF2 activity is not restricted to cases of PC

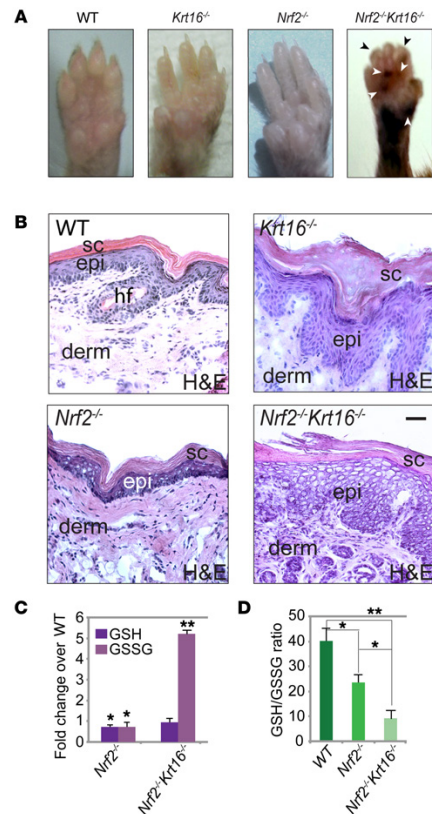


**Figure 4. Loss of NRF2 results in earlier onset of hyperkeratotic front paw calluses in *Krt16*<sup>-/-</sup> mice.** Images (A) and H&E staining (B) of representative front paws from male 1-month-old WT, *Krt16*<sup>-/-</sup>, *Nrf2*<sup>-/-</sup>, and *Nrf2*<sup>-/-</sup>*Krt16*<sup>-/-</sup> mice. hf, hair follicle. White arrows mark hyperpigmented calluses; black arrowheads mark contracted digits. Scale bar: 50  $\mu$ m. (C) Fold change in GSH and GSSG for *Nrf2*<sup>-/-</sup> and *Nrf2*<sup>-/-</sup>*Krt16*<sup>-/-</sup> paw skin relative to WT. Data represent mean  $\pm$  SEM of 6 biological replicates, Student's *t* test. (D) GSH/GSSG ratio for WT, *Nrf2*<sup>-/-</sup>, and *Nrf2*<sup>-/-</sup>*Krt16*<sup>-/-</sup> paw skin. Data represent mean  $\pm$  SEM of 6 biological replicates. ANOVA. \**P* < 0.05; \*\**P* < 0.01.

the *Nrf2*<sup>-/-</sup> mice, the *Nrf2*<sup>-/-</sup>*Krt16*<sup>-/-</sup> mice also exhibited striking vacuolar changes in the epidermis (Figure 4B). Moreover, at 1 month of age, the ventral surfaces of *Nrf2*<sup>-/-</sup>*Krt16*<sup>-/-</sup> mice were remarkable for areas of hyperkeratosis, alopecia, and extensive eschar (Supplemental Figure 3). The dorsal surfaces of the *Nrf2*<sup>-/-</sup>*Krt16*<sup>-/-</sup> mice also exhibited thinning hair and patches of erythema (Supplemental Figure 3). These findings establish the existence of a functional link between K16 and NRF2 in skin keratinocytes. We also assessed the levels of GSH and GSSG in paw tissue taken from 1-month-old *Nrf2*<sup>-/-</sup> and *Nrf2*<sup>-/-</sup>*Krt16*<sup>-/-</sup> male mice. GSH and GSSG levels, as well as the GSH to GSSG ratio, were decreased in *Nrf2*<sup>-/-</sup> paw skin, which indicates increased oxidative stress relative to WT paw skin. The loss of both *Nrf2* and *Krt16* has an even more dramatic impact on redox balance. GSH is  $1.4 \pm 0.23$ -fold lower in *Nrf2*<sup>-/-</sup>*Krt16*<sup>-/-</sup> paw skin, but GSSG is approximately 5-fold higher than WT (Figure 4C; mean  $\pm$  SEM). There was also significant effect of genotype on the GSH to GSSG ratio (ANOVA, *P* = 0.0001). In the absence of both *Nrf2* and *Krt16*, the GSH to GSSG ratio dropped to a remarkably low  $9.08 \pm 3.58$  relative to  $40.1 \pm 5.2$  and  $23.5 \pm 3.2$  for WT and *Nrf2*<sup>-/-</sup>, respectively (Figure 4D; mean  $\pm$  SEM).

Second, this hypothesis predicts that expression of K16 in cultured skin keratinocytes should enhance NRF2 activity. To test this prediction, we transfected immortalized 308 mouse skin keratinocytes that have low endogenous *Krt16* expression with construct encoding either GFP-fused K16 or GFP-fused K14, used here for comparison, and evaluated the subcellular localization and phosphorylation status of NRF2 by indirect immunofluorescence. Marked increases in nuclear-localized NRF2 and p-NRF2 (by  $2.2 \pm 0.75$ -fold and  $5.3 \pm 0.48$ -fold, respectively) were detected in cells expressing GFP-K16 relative to those expressing GFP-K14 (Figure 5, A and B; *n* = 40 cells per group, mean  $\pm$  SEM). These findings suggest that, relative to K14, K16 exhibits a significantly stronger ability to enhance NRF2 function in skin keratinocytes.

Third, we probed for a potential mechanism through which K16 could influence PKC $\delta$  expression and activation in cultured skin keratinocytes. The receptor for activated C kinase 1 (RACK1) has been shown to stabilize the active conformation of PKCs, including the PKC $\delta$  isoform, and act as a shuttling protein (26). Intriguingly, K5 and K14 have been shown by others to physically interact with RACK1, leading to its sequestration and the inhibition of PKC $\alpha$  activity (27). We hypothesized that, unlike the basal-specific K5/K14, K16 would not interact with and/or sequester RACK1 in keratinocytes. Consistent with previous findings (27), substantial colocalization of RACK1 and K14 was observed in 308 mouse skin keratinocytes in culture. In contrast, faint or no colocalization of RACK1 and K16 was detected in 308 cells that were transfected with GFP-fused K16 (Figure 5C).

arising from mutations in *KRT16*, though a full exploration of this important issue will require studies on additional PPK/PC biopsies.

**Substantiating the link between K16 and NRF2 activation.** We next conducted several experiments to test the hypothesis that *Krt16*/K16 plays a significant role in regulating NRF2 activity in skin keratinocytes. First, this hypothesis predicts that the *Krt16*<sup>-/-</sup> skin phenotype should worsen in the setting of a complete NRF2 deficiency. To test this prediction, we mated the *Krt16*<sup>-/-</sup> mice with *Nrf2*<sup>-/-</sup> mice (available in the same genetic background) and assessed the onset of paw lesions and overall skin appearance in the resulting offspring. Representative images of paws from *Krt16*<sup>-/-</sup>, *Nrf2*<sup>-/-</sup>, and *Nrf2*<sup>-/-</sup>*Krt16*<sup>-/-</sup> mice are shown in Figure 4A. Of the *Nrf2*<sup>-/-</sup>*Krt16*<sup>-/-</sup> mice that were monitored (*n* = 20), approximately 50% died by P1 and the remaining 50% developed hyperkeratotic calluses and digital contractures by 3 weeks of age. This is 3 weeks earlier than the average age of onset for clinically evident paw lesions in *Krt16*<sup>-/-</sup> mice (13). Similarly to the *Krt16*<sup>-/-</sup> mice, the *Nrf2*<sup>-/-</sup>*Krt16*<sup>-/-</sup> mice had thickened epidermis and stratum corneum at 1 month of age. Like

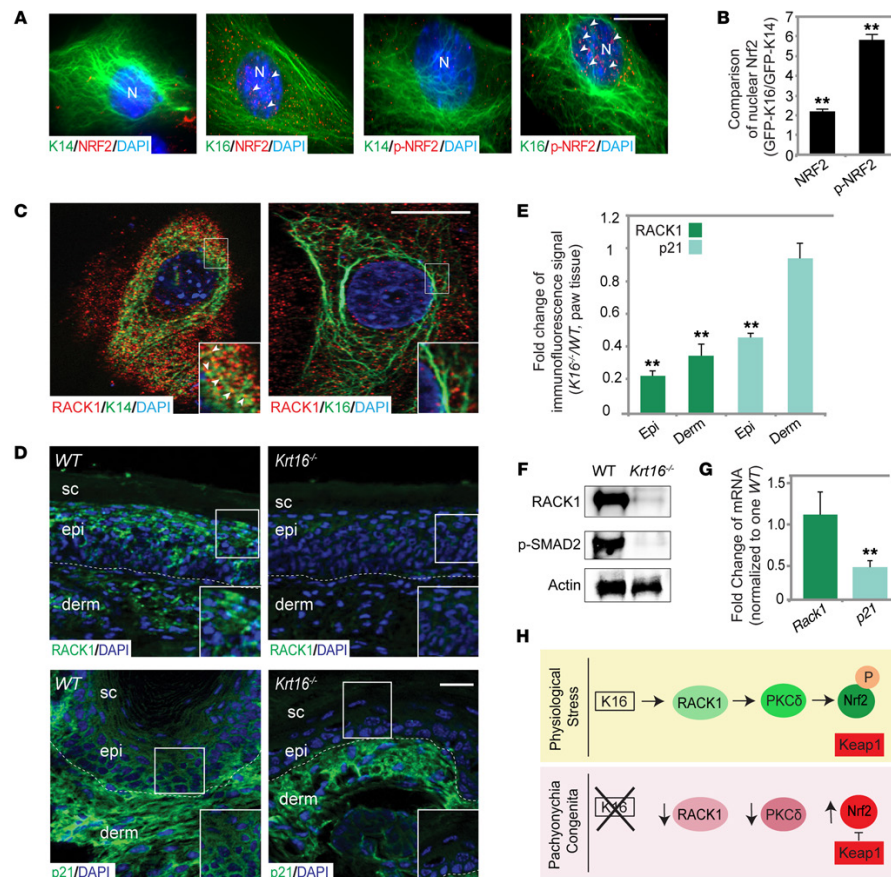
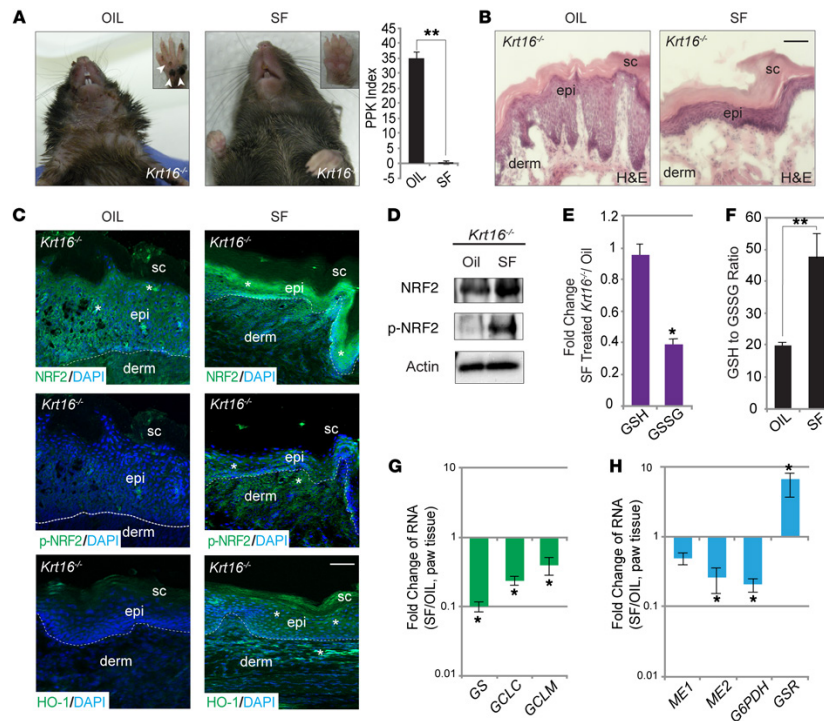


**Figure 5. A link between *Krt16* and NRF2 activation.** (A) Indirect immunofluorescence for NRF2 and p-NRF2 in 308 cells transfected with GFP-fused K14 or K16. Scale bar: 10  $\mu$ m. Arrowheads mark increased nuclear immunofluorescence signal. N, nucleus. (B) Quantitation of intranuclear NRF2 and p-NRF2 immunofluorescence signal. Data represent mean  $\pm$  SEM for 40 cells per group normalized for nuclear size. Student's *t* test. (C) Indirect immunofluorescence for RACK1 in 308 cells transfected with GFP-fused K16. Scale bar: 10  $\mu$ m; 100  $\mu$ m (inset). (D) Indirect immunofluorescence for RACK1 and p21 in paw skin of 1-month-old male mice. Dotted lines mark dermoepidermal junction. Scale bar: 50  $\mu$ m; 100  $\mu$ m (inset). (E) Relative fold change of immunofluorescence signal for WT and *Krt16*<sup>-/-</sup> paw tissue stained for RACK1 and p21. Data represent mean  $\pm$  SEM of 10 mice, 2 images per mouse. Student's *t* test. (F) Representative Western blot for RACK1 and p-SMAD2 of 3 experiments with actin as loading control. (G) Fold change of mRNA for *Rack1* and *p21* in prelesional paw skin of *Krt16*<sup>-/-</sup> mice relative to WT. Data represent mean  $\pm$  SEM of 4 biological replicates. Student's *t* test. (H) Schematic of proposed regulation of NRF2 pathway in the suprabasal epidermis under normal physiological conditions and without K16. \*\**P* < 0.01.

Fourth, we measured the levels of RACK1 protein in prelesional *Krt16*<sup>-/-</sup> paw tissue in order to assess the physiological consequence of the lack of physical interaction between K16 and RACK1 uncovered in cultured keratinocytes. RACK1 is a known NRF2 target (28) and, accordingly, its levels should be depressed given the markedly hypoactive character of the latter in *Krt16*<sup>-/-</sup> footpad skin. Relative to control skin, there was a marked reduction of

RACK1 protein, as detected by indirect immunofluorescence (Figure 5, D and E) and Western blotting (Figure 5F). Similarly to p-NRF2 (Ser-40) and its downstream targets, RACK1 was diminished in both the epidermis and the dermis of *Krt16*<sup>-/-</sup> skin (by  $4.34 \pm 0.03$ -fold and  $2.9 \pm 0.10$ -fold, respectively) (Figure 5E). In contrast to the protein, *Rack1* mRNA levels remained comparable to those of control (Figure 5G).



Another mechanism of interest regarding NRF2 activation in skin keratinocytes consists of the TGF- $\beta$ -dependent transcriptional activation of p21, which was recently shown to stabilize NRF2 and enhance GSH metabolism (29). Interestingly, we found that p21 protein levels were decreased by 2-fold in *Krt16*<sup>-/-</sup> epidermis (Figure 5, D and E) and mRNA levels were decreased by 2-fold in total paw skin (Figure 5G). Protein levels of p-SMAD2, a key terminal effector of the TGF- $\beta$  signaling pathway, were also lower in *Krt16*<sup>-/-</sup> skin versus WT control (Figure 5F). Since overexpression of RACK1 in NIH 3T3 cells has been correlated with increased p21 expression (30) and RACK1 has been shown to both promote and be a target of TGF- $\beta$ 1 signaling in fibrotic liver (31), the reduction in p21 levels and the impairment of TGF- $\beta$  signaling in *Krt16*<sup>-/-</sup> skin may be related to the decrease of RACK1. These results point to the existence of a connection among K16, TGF- $\beta$

signaling, RACK1 protein synthesis and/or stability, PKC $\delta$  activity, and p21 transcription, all of which are capable of significantly affecting NRF2 activity in the suprabasal epidermis under stress conditions. We hypothesize that K16, either through a competitive effect on the sequestration of RACK1 by K14 and K5 or a still unclear mechanism, promotes the stabilization of RACK1, which ultimately results in NRF2 activation that is confined to the suprabasal layer (Figure 5H).

**Small molecule-based activation of NRF2 rescues PPK in *Krt16*<sup>-/-</sup> mice.** To further the relevance of NRF2's markedly attenuated activity in the development of the hyperkeratotic calluses in *Krt16*<sup>-/-</sup> mice, we topically treated 1-month-old male *Krt16*<sup>-/-</sup> mice with sulforaphane (SF), an NRF2 inducer derived from broccoli sprout extract (32), twice weekly for 4 consecutive weeks. This seemed a plausible approach given the high amounts of NRF2 protein avail-

able for activation in *Krt16*<sup>-/-</sup> skin. Remarkably, significantly fewer hyperpigmented calluses were observed in SF-treated *Krt16*<sup>-/-</sup> paws (Figure 6A). A blinded assessment (Supplemental Figure 4) ascertained that the average affected surface area of SF-treated paws was dramatically lower ( $0.08\% \pm 0.07\%$  in SF-treated versus  $34.9\% \pm 3.2\%$  for vehicle-treated paws; mean  $\pm$  SEM;  $n = 10$  mice per experimental group) (Figure 6A). Histologically, the extent of epidermal thickening was markedly less in SF-treated paw tissue relative to vehicle treated (Figure 6B). As anticipated, increased indirect immunofluorescence signals for NRF2, p-NRF2 (Ser40), and HO-1 occurred in both the epidermis and dermis of SF-treated *Krt16*<sup>-/-</sup> paws (Figure 6C). The increases in NRF2 and p-NRF2 were confirmed with Western blotting (Figure 6D). Indirect immunofluorescence signals for RACK1, PKC $\delta$ , and p-PKC $\delta$  were also increased in the epidermis of *Krt16*<sup>-/-</sup> paws following SF treatment (Supplemental Figure 5). These results suggest that topical treatment with SF successfully activated NRF2 in *Krt16*<sup>-/-</sup> paw skin tissue. Strikingly, GSH levels were similar in *Krt16*<sup>-/-</sup> mice whether they were treated with SF or vehicle ( $0.96 \pm 0.07$ -fold change; mean  $\pm$  SEM); however, GSSG levels were diminished  $2.56 \pm 0.05$ -fold following SF treatment (Figure 6E; mean  $\pm$  SEM). This resulted in decreased oxidative stress overall, as indicated by a higher GSH to GSSG ratio ( $47.1 \pm 7.8$  in SF-treated versus  $19.9 \pm 0.9$  in vehicle-treated *Krt16*<sup>-/-</sup> paw tissue) (Figure 6F; mean  $\pm$  SEM). After SF treatment, the mRNA levels of *Gss*, *Gclc*, *Gclm*, *Me1/2*, and *G6pd* were down, but there was a significant,  $6.6 \pm 2.4$ -fold, rise in *Gsr* mRNA (Figure 6, G and H; mean  $\pm$  SEM). Taken together, these unexpected findings imply that topical treatment with SF improves regeneration of GSH, but GSH synthesis remains defective in skin lacking K16.

## Discussion

We previously reported that *Krt16*<sup>-/-</sup> mice develop footpad lesions that histologically and molecularly mimic PC-associated PPK (13). In the present study, we determined that there is increased oxidative stress associated with an impairment of GSH synthesis, prior to lesion onset, in *Krt16*<sup>-/-</sup> paw skin. This oxidative stress, by itself or as a trigger of cell/tissue damage, is poised to play a significant role in the phenomenon of increased expression of DAMPs and innate immunity markers. It may also stimulate regulators of the skin barrier in *Krt16*<sup>-/-</sup> paw skin (11) and originates, to a substantial degree, from the dysfunction of the KEAP1/NRF2 signaling pathway. In vitro and in vivo experiments revealed a connection between *Krt16* expression and activation of NRF2, as assessed via nuclear localization, phosphorylation status, and expression of key target genes. Two important upstream regulators of NRF2 activity, RACK1 and PKC $\delta$ , were found to be hypoactive and/or decreased in *Krt16*<sup>-/-</sup> paw skin. Genetic ablation of *Nrf2* resulted in an earlier onset of PPK lesions in *Krt16*<sup>-/-</sup> mice, whereas topical treatment with the NRF2 activator SF prevented lesion formation and restored redox balance to near normal in *Krt16*<sup>-/-</sup> mice, confirming the significance of the NRF2 pathway in the pathophysiology of hyperkeratotic paw calluses. Finally, we provided evidence that NRF2 can be readily detected but is hypophosphorylated, reflecting low activity, in lesional plantar skin tissue of individuals with PC, lending strong support to the relevance and significance of the observations made in the *Krt16*-null mouse model.

Our results suggest a role for K16 in defining the skin's response to oxidative stress through the modulation of the NRF2 signaling pathway. NRF2 is constitutively expressed in keratinocytes of normal skin and is upregulated upon wounding and exposure to electrophiles (33). Following UVB irradiation, NRF2 activates the production and export of GSH by suprabasal keratinocytes, which subsequently protect basal keratinocytes in a paracrine manner (34). We show here that the loss of *Krt16*, whose expression in glabrous skin is normally limited to the suprabasal compartment, selectively affects GSH production. Thus, rather than a global impact on NRF2 signaling, K16 appears to regulate a subset of the NRF2 transcriptional program. Unlike the basal-specific keratins K5 and K14, K16 does not appear to sequester RACK1 and subsequently inhibit PKC activation. In the absence of K16, in fact, RACK1 protein levels and p-PKC $\delta$  are markedly lower in glabrous skin. TGF- $\beta$  signaling through SMAD2 is also impaired, and levels of p21 are reduced in skin lacking K16. Taken together, these findings imply that K16, whose expression can be stimulated by TGF- $\beta$  in cultured keratinocytes (35), may be involved in a complex signaling network involving TGF- $\beta$ , p21, RACK1, and NRF2 that ultimately affects redox balance in skin keratinocytes. The positive impact of K16 on TGF- $\beta$  signaling may, under normal conditions, contribute to the suprabasal-to-basal gradient of NRF2 (and its target genes) brought to light by Schafer et al. following UVB irradiation (34). This suggests that K16 is poised to be a key contributor to the unique cellular redox capabilities of the suprabasal compartment of epidermis in glabrous skin. Interestingly, *Krt16* is an NRF2 target gene (19, 21). The role of K16 toward NRF2 activation shown in this study suggests that it powers a positive feedback loop toward the regulation of NRF2 function in skin keratinocytes. We recently showed that the related K17 acts in a similar fashion with regard to the expression of proinflammatory cytokines in tumor-prone skin keratinocytes, achieved through its interaction with the ribonucleoprotein heterogeneous nuclear ribonucleoprotein K (hnRNP K) (36).

Our findings extend the current understanding of the pathogenesis of the painful and debilitating PPK associated with PC and provide compelling evidence that the noncanonical functions of keratins represent therapeutic targets for keratin-based disorders. We provide evidence in the current study that NRF2 function is likely compromised in lesional PPK-stricken plantar skin tissue from individuals with PC. Whether alterations in GSH metabolism and oxidative stress occur in the setting of PPK in individuals with PC and whether these findings are also relevant to the pathogenesis of related skin disorders are open issues of great significance. Besides, current treatment strategies for PC focus on silencing of the affected keratin genes and have yielded mixed results (37–40). Simply silencing mutant keratin gene expression may be insufficient for an effective treatment of PC, and at the very least, a combination of gene silencing and a pharmacological restoration of redox balance and NRF2 signaling may be required to achieve a significant clinical improvement of PPK. SF, particularly in its natural form as broccoli sprout extract, is clinically attractive as a pharmacological NRF2 inducer given several previous studies demonstrating the safety of topical use in murine and human skin (41–43). On a different level, SF could exert NRF2-independent effects that contribute to the rescue of the *Krt16*<sup>-/-</sup> mice, a possibility that deserves

further investigation and that may add to the clinical benefit of the application of SF in PC. Also of interest, the antioxidant effects of NRF2 extend well beyond GSH metabolism and also include, for instance, a stimulation of mitochondrial biogenesis, metabolism, and function (44, 45). Such elements may contribute to the pathogenesis of PPK lesions and as such represent additional therapeutic targets of interest in PC and related disorders.

In a broader context, an enhanced understanding of the pathophysiology of PC opens up new therapeutic avenues for more common deficiencies in wound healing that plague clinical practice today. Given that it arises from mutations in wound-inducible keratins and is associated with an impairment of cellular stress responses, PC possibly represents a genetically determined disorder in which wound healing is markedly impaired. The lessons learned regarding the role of keratins in the regulation of redox balance in the course of investigating PC may be applicable to additional conditions in which oxidative stress plays a key role, e.g., diabetic wound ulcers and nonhealing chronic wounds. Pharmacological manipulation of redox balance and/or keratin expression may also provide a viable treatment approach for these challenging maladies.

## Methods

**Animals, antibodies, and preparation of SF.** *Krt16*<sup>-/-</sup> and *Nrf2*<sup>-/-</sup> mouse lines on a C57BL/6 background were maintained under specific pathogen-free conditions and fed chow and water ad libitum. *Krt16*<sup>-/-</sup> mice were generated by our laboratory (13). *Nrf2*<sup>-/-</sup> mice were provided by Thomas Kensler (Johns Hopkins University). Commercial antibodies used are listed in Supplemental Table 1. Generation of the K16 antibody has been described (46). Alexa Fluor-conjugated secondary antibodies as well as goat anti-mouse and goat anti-rabbit (Life Technologies) antibodies were also used. SF was obtained from LKT Laboratories Inc. Stock solutions of SF were prepared at 0.1 M in DMSO vehicle. For topical application, SF was diluted to the desired final concentration in jojoba oil (MP Biomedicals LLC) on the day of the treatment, as described (19, 43).

**Mouse and cell culture studies.** Four- and 6-week-old *Krt16*<sup>-/-</sup> or WT male mice were topically treated with either 100  $\mu$ l of 1  $\mu$ M SF or vehicle control on their front paws twice weekly for 4 weeks. Upon completion of the treatment regimen, the ventral surface of each treated paw was photographed, and the extent of PPK-like lesions was blindly and independently assessed by 5 individuals as described in Supplemental Figure 2.

Four-week-old WT mice were given i.p. injections of 50  $\mu$ M BSO (Sigma-Aldrich), an inhibitor of GSH synthesis, in PBS or PBS alone twice weekly (19). The mice were harvested after 4 weeks; levels of GSH and GSSG levels in paw tissue were assessed, and histological analysis was performed.

The 308 mouse epidermal keratinocytes (47) were cultured in DMEM (Invitrogen) containing 10% FBS (Atlanta Biologicals), 100 units/ml penicillin, and 100  $\mu$ g/ml streptomycin (Invitrogen) at 37°C in 5% CO<sub>2</sub>. GFP-K16 was transiently transfected using FuGENE HD transfection reagent (Promega) according to the manufacturer's protocol. Indirect immunofluorescence was performed as described (48). GFP-K16- or GFP-K14-transfected 308 mouse epidermal keratinocytes were fixed in 4% paraformaldehyde for 10 minutes at room temperature, washed in PBS, blocked in 5% normal goat serum/0.1% Triton X-100/PBS for 1 hour at room temperature, incubated in primary antibody

solution for 1 hour, washed in PBS, incubated in secondary antibody solution for 1 hour, counterstained with DAPI, and mounted in Fluor-Save Reagent Mounting Medium (EMD Millipore) before visualization using a Zeiss fluorescence microscope with an ApoTome attachment.

**Human studies.** Punch biopsies (3 mm) from PC patients were obtained as previously described (48) and analyzed for protein expression by immunohistochemistry. Cryosections (10  $\mu$ m) were fixed with ice-cold acetone for 20 minutes, washed with PBS, and incubated with 2% BSA in PBS for 1 hour at room temperature to minimize nonspecific binding. The sections were incubated overnight at 4°C in primary antibody solution, washed in PBS, and incubated in secondary antibody solution for 1 hour. Following counterstaining with DAPI and mounting in Hydromount (National Diagnostics), protein expression was visualized using a Zeiss fluorescence microscope.

**Biochemical and morphological analysis.** RNA was extracted from front paws using TRIzol reagent (Life Technologies). After DNase treatment (RNase free DNase kit: QIAGEN), 1  $\mu$ g of total RNA from each sample was reverse transcribed (iScript cDNA synthesis kit; Bio-Rad). Quantitative RT-PCR was performed as described (49). The target-specific oligonucleotide primer sets used are listed in Supplemental Table 2. For protein analyses, paw tissue was homogenized and extracted using TRIzol reagent (Life Technologies). Protein concentration was measured using a Bradford Assay Kit (Bio-Rad). Equal amounts of protein (15–20  $\mu$ g range) were loaded onto 10% SDS/PAGE gels and blotted onto nitrocellulose. Actin was used as a loading control in all immunoblots. Bound primary antibodies were detected with enhanced chemiluminescence (Thermo Scientific). GSH and GSSG levels in skin tissue were assessed using a Glutathione Fluorometric assay kit from BioVision. NADPH levels were measured using a colorimetric kit (BioVision). For histological analyses, paw tissue samples were submerged in OCT (Sakura Finetek), flash-frozen in liquid nitrogen, and stored at -20°C upon sectioning. Sections of 8  $\mu$ m were cut in a specific and consistent orientation relative to paw morphology and stained with either H&E for routine histopathology or incubated with primary antibodies and Alexa Fluor-conjugated secondary antibodies for indirect immunofluorescence (49).

**Statistics.** Unpaired 2-tailed Student's *t* test and ANOVA were performed when appropriate. Significant differences between 2 groups were noted by asterisks. Quantification data were presented in mean  $\pm$  SEM. Blinded quantitation of indirect IF was performed using ImageJ (NIH).

**Study approval.** All studies involving mice were approved by the Johns Hopkins University Institutional Animal Care and Use Committee. Human plantar skin biopsies were obtained using standard surgical techniques with patient consent under W-IRB #2004/0468/1057496 (47).

## Author contributions

MLK, JMCH, RGL, and YG conducted all experiments and assisted with the analysis and interpretation of the data. MLK and PAC designed the experiments and wrote the manuscript. AB and RLK played a key role in generating the human data. All authors read and commented on the manuscript.

## Acknowledgments

The authors thank Mary Schwartz and David C. Hansen from the Pachonychia Congenita Project ([www.pachonychia.org](http://www.pachonychia.org)) and members of the Coulombe laboratory for support; PC patients and nonpatient volunteers for providing biopsies; Michael Polydefkis,

Baohan Pan, and Madelyn Low for assistance; Christopher Contag for support; and Juliane Lessard and Tom Kensler for advice. This work was supported by RO1 grant AR44232 (to P.A. Coulombe) from the NIH. M.L. Kerns received support from T32 training grant CA009110 from the NIH.

Address correspondence to: Pierre A. Coulombe, Department of Biochemistry and Molecular Biology, Johns Hopkins Bloomberg School of Public Health, 615 N. Wolfe Street, Room W8041, Baltimore, Maryland 21205, USA. Phone: 410.955.3671; E-mail: coulombe@jhu.edu.

- Coulombe PA, Hutton ME, Vassar R, Fuchs E. A function for keratins and a common thread among different types of epidermolysis bullosa simplex diseases. *J Cell Biol.* 1991;115(6):1661-1674.
- Omary MB, Coulombe PA, McLean WH. Intermediate filament proteins and their associated diseases. *N Engl J Med.* 2004;351(20):2087-2100.
- Szevenyi I, et al. The Human Intermediate Filament Database: comprehensive information on a gene family involved in many human diseases. *Hum Mutat.* 2008;29(3):351-360.
- Coulombe PA, Kerns ML, Fuchs E. Epidermolysis bullosa simplex: a paradigm for disorders of tissue fragility. *J Clin Invest.* 2009;119(7):1784-1793.
- Pan X, Hobbs RP, Coulombe PA. The expanding significance of keratin intermediate filaments in normal and diseased epithelia. *Curr Opin Cell Biol.* 2013;25(1):47-56.
- Hamada T, et al. How do keratinizing disorders and blistering disorders overlap? *Exp Dermatol.* 2013;22(2):83-87.
- Smith FJ, et al. The genetic basis of pachyonychia congenita. *J Invest Dermatol Symp Proc.* 2005;10(1):21-30.
- McLean WH, et al. Keratin 16 and keratin 17 mutations cause pachyonychia congenita. *Nat Genet.* 1995;9(3):273-278.
- McGowan K, Coulombe PA. The wound repair-associated keratins 6, 16, and 17. *Subcell Biochem.* 1998;31:173-204.
- Eliason MJ, Leachman SA, Feng BJ, Schwartz ME, Hansen CD. A review of the clinical phenotype of 254 patients with genetically confirmed pachyonychia congenita. *J Am Acad Dermatol.* 2012;67(4):680-686.
- Lessard JC, et al. Keratin 16 regulates innate immunity in response to epidermal barrier breach. *Proc Natl Acad Sci U S A.* 2013;110(48):19537-19542.
- Shah S, Boen M, Kenner-Bell B, Schwartz M, Rademaker A, Paller AS. Pachyonychia congenita in pediatric patients: natural history, features, and impact. *JAMA Dermatol.* 2014;150(2):146-153.
- Lessard JC, Coulombe PA. Keratin 16-null mice develop palmoplantar keratoderma, a hallmark feature of pachyonychia congenita and related disorders. *J Invest Dermatol.* 2012;132(5):1384-1391.
- Lushchak VI. Glutathione homeostasis and functions: potential targets for medical interventions. *J Amino Acids.* 2012;2012:736837.
- Pastore A, et al. Determination of blood total, reduced, and oxidized glutathione in pediatric subjects. *Clin Chem.* 2001;47(8):1467-1469.
- Dalton TP, Dieter MZ, Yang Y, Shertzer HG, Nebert DW. Knockout of the mouse glutamate cysteine ligase catalytic subunit (Gcl) gene: embryonic lethal when homozygous, and proposed model for moderate glutathione deficiency when heterozygous. *Biochem Biophys Res Commun.* 2000;279(2):324-329.
- Yang Y, Dieter MZ, Chen Y, Shertzer HG, Nebert DW, Dalton TP. Initial characterization of the glutamate-cysteine ligase modifier subunit Gclm(-/-) knockout mouse. *J Biol Chem.* 2002;277(51):49446-49452.
- Couto N, Malys N, Gaskell SJ, Barber J. Partition and turnover of glutathione reductase from *Saccharomyces cerevisiae*: a proteomic approach. *J Proteome Res.* 2013;12(6):2885-2894.
- Kerns M, DePianto D, Yamamoto M, Coulombe PA. Differential modulation of keratin expression by sulforaphane occurs via Nrf2-dependent and -independent pathways in skin epithelia. *Mol Biol Cell.* 2010;21(23):4068-4075.
- Gorini C, Harris IS, Mak TW. Modulation of oxidative stress as an anticancer strategy. *Nat Rev Drug Discov.* 2013;12(12):931-947.
- Endo H, Sugioaka Y, Nakagi Y, Saijo Y, Yoshida T. A novel role of the Nrf2 transcription factor in the regulation of arsenite-mediated keratin 16 gene expression in human keratinocytes. *Environ Health Perspect.* 2008;116(7):873-879.
- Alam J, Cook JL. Transcriptional regulation of the heme oxygenase-1 gene via the stress response element pathway. *Curr Pharm Des.* 2003;9(30):2499-2511.
- Kwak MK, Itoh K, Yamamoto M, Sutter TR, Kensler TW. Role of transcription factor Nrf2 in the induction of hepatic phase 2 and antioxidant enzymes in vivo by the cancer chemoprotective agent, 3H-1, 2-dimethiole-3-thione. *Mol Med.* 2001;7(2):135-145.
- Itoh K, et al. Keap1 represses nuclear activation of antioxidant responsive elements by Nrf2 through binding to the amino-terminal Neh2 domain. *Genes Dev.* 1999;13(1):76-86.
- Niture SK, Jain AK, Jaiswal AK. Antioxidant-induced modification of INrf2 cysteine 151 and PKC-delta-mediated phosphorylation of Nrf2 serine 40 are both required for stabilization and nuclear translocation of Nrf2 and increased drug resistance. *J Cell Sci.* 2009;122(pt 24):4452-4464.
- Adams DR, Ron D, Kiely PA. RACK1, A multifaceted scaffolding protein: structure and function. *Cell Commun Signal.* 2011;9:22.
- Kroger C, Loschke F, Schwarz N, Windoffer R, Leube RE, Magin TM. Keratins control intercellular adhesion involving PKC- $\alpha$ -mediated desmoplakin phosphorylation. *J Cell Biol.* 2013;201(5):681-692.
- Kim YH, Coon A, Baker AF, Powis G. Antitumor agent PX-12 inhibits HIF-1 $\alpha$  protein levels through an Nrf2/PMF-1-mediated increase in spermidine/spermine acetyl transferase. *Cancer Chemother Pharmacol.* 2011;68(2):405-413.
- Oshimori N, Oristian D, Fuchs E. TGF- $\beta$  promotes heterogeneity and drug resistance in squamous cell carcinoma. *Cell.* 2015;160(5):963-976.
- Hermanto Y, Zong CS, Li W, Wang LH. RACK1, an insulin-like growth factor I (IGF-I) receptor-interacting protein, modulates IGF-I-dependent integrin signaling and promotes cell spreading and contact with extracellular matrix. *Mol Cell Biol.* 2002;22(7):2345-2365.
- Jia D, et al. Up-regulation of RACK1 by TGF- $\beta$ 1 promotes hepatic fibrosis in mice. *PLoS One.* 2013;8(3):e60115.
- Zhang Y, Talalay P, Cho CG, Posner GH. A major inducer of anticarcinogenic protective enzymes from broccoli: isolation and elucidation of structure. *Proc Natl Acad Sci U S A.* 1992;89(6):2399-2403.
- Braun S, et al. Nrf2 transcription factor, a novel target of keratinocyte growth factor action which regulates gene expression and inflammation in the healing skin wound. *Mol Cell Biol.* 2002;22(15):5492-5505.
- Schafer M, Dutsch S, auf dem Keller U, Werner S. Nrf2: a central regulator of UV protection in the epidermis. *Cell Cycle.* 2010;9(15):2917-2918.
- Choi Y, Fuchs E. TGF- $\beta$  and retinoic acid: regulators of growth and modifiers of differentiation in human epidermal cells. *Cell Regul.* 1990;1(11):791-809.
- Chung BM, Arutyunov A, Ilagan E, Yao N, Wills-Karp M, Coulombe PA. Regulation of C-X-C chemokine gene expression by keratin 17 and hnRNP K in skin tumor keratinocytes. *J Cell Biol.* 2015;208(5):613-627.
- Goldberg I, Fruchter D, Mellick A, Schwartz ME, Sprecher E. Best treatment practices for pachyonychia congenita. *J Eur Acad Dermatol Venerol.* 2014;28(3):279-285.
- Leachman SA, et al. First-in-human mutation-targeted siRNA phase Ib trial of an inherited skin disorder. *Mol Ther.* 2010;18(2):442-446.
- Milstone LM, et al. Treatment of pachyonychia congenita. *J Invest Dermatol Symp Proc.* 2005;10(1):18-20.
- Trochet D, Prudhon B, Vassilopoulos S, Bitoun M. Therapy for dominant inherited diseases by allele-specific RNA interference: successes and pitfalls. *Curr Gene Ther.* 2015;15(5):503-510.
- Kerns ML, DePianto D, Dinkova-Kostova AT, Talalay P, Coulombe PA. Reprogramming of keratin biosynthesis by sulforaphane restores skin integrity in epidermolysis bullosa simplex. *Proc Natl Acad Sci U S A.* 2007;104(36):14460-14465.
- Dinkova-Kostova AT, et al. Protection against UV-light-induced skin carcinogenesis in SKH-1 high-risk mice by sulforaphane-containing broccoli sprout extracts. *Cancer Lett.* 2006;240(2):243-252.
- Dinkova-Kostova AT, et al. Induction of the phase 2 response in mouse and human skin by sulforaphane-containing broccoli sprout extracts. *Cancer Epidemiol Biomarkers Prev.* 2007;16(4):847-851.
- MacGarvey NC, Suliman HB, Bartz RR, Fu P, Withers CM, KE Piantadosi CA. Activation of

RESEARCH ARTICLE

The Journal of Clinical Investigation

- mitochondrial biogenesis by heme-oxygenase-1-mediated NF-E2-related factor-2 induction rescues mice from lethal *Staphylococcus aureus* sepsis. *Am J Respir Crit Care Med*. 2012;185(8):851–861.
45. Tufekci KU, Civi Bayin E, Gene S, Gene K. The Nrf2/ARE pathway: a promising target to counteract mitochondrial dysfunction in Parkinson's disease. *Parkinsons Dis*. 2011;2011:314082.
46. Bernot KM, Coulombe PA, McGowan KM. Keratin 16 expression defines a subset of epithelial cells during skin morphogenesis and the hair cycle. *J Invest Dermatol*. 2002;119(5):1137–1149.
47. Strickland JE, et al. Development of murine epidermal cell lines which contain an activated rasHa oncogene and form papillomas in skin grafts on athymic nude mouse hosts. *Cancer Res*. 1988;48(1):165–169.
48. Seegmiller BL. Gene expression profiling in pachyonychia congenita skin. *J Dermatol Sci*. 2015;77(3):156–165.
49. Hobbs RP, et al. Keratin-dependent regulation of Aire and gene expression in skin tumor keratinocytes. *Nat Genet*. 2015;47(8):933–938.

## REFERENCES

- Adams, D. R., Ron, D., & Kiely, P. A. (2011). RACK1, A multifaceted scaffolding protein: Structure and function. *Cell Communication and Signaling*, 9(1), 1.
- Alam, J., & Cook, J. (2003). Transcriptional regulation of the heme oxygenase-1 gene via the stress response element pathway. *Current Pharmaceutical Design*, 9(30), 2499-2511.
- Ansell, P., Lo, S., Newton, L., Espinosa-Nicholas, C., Zhang, D., Liu, J., et al. (2005). Repression of cancer protective genes by 17 $\beta$ -estradiol: Ligand-dependent interaction between human Nrf2 and estrogen receptor  $\alpha$ . *Molecular and Cellular Endocrinology*, 243(1), 27-34.
- Braun, S., Hanselmann, C., Gassmann, M. G., auf dem Keller, U., Born-Berclaz, C., Chan, K., et al. (2002). Nrf2 transcription factor, a novel target of keratinocyte growth factor action which regulates gene expression and inflammation in the healing skin wound. *Molecular and Cellular Biology*, 22(15), 5492-5505.
- Campbell, L., Emmerson, E., Davies, F., Gilliver, S. C., Krust, A., Chambon, P., et al. (2010). Estrogen promotes cutaneous wound healing via estrogen receptor beta independent of its antiinflammatory activities. *The Journal of Experimental Medicine*, 207(9), 1825-1833.
- Chan, Y., Anton-Lamprecht, I., Yu, Q. C., Jackel, A., Zabel, B., Ernst, J. P., et al. (1994). A human keratin 14 "knockout": The absence of K14 leads to severe epidermolysis bullosa simplex and a function for an intermediate filament protein. *Genes & Development*, 8(21), 2574-2587.

- Chen, W., Sun, Z., Wang, X., Jiang, T., Huang, Z., Fang, D., et al. (2009). Direct interaction between Nrf2 and p21 Cip1/WAF1 upregulates the Nrf2-mediated antioxidant response. *Molecular Cell*, 34(6), 663-673.
- Choi, Y., & Fuchs, E. (1990). TGF-beta and retinoic acid: Regulators of growth and modifiers of differentiation in human epidermal cells. *Cell Regulation*, 1(11), 791-809.
- Coulombe, P. A., & Omary, M. B. (2002). 'Hard' and 'soft' principles defining the structure, function and regulation of keratin intermediate filaments. *Current Opinion in Cell Biology*, 14(1), 110-122.
- Coulombe, P. A., Kerns, M. L., & Fuchs, E. (2009). Epidermolysis bullosa simplex: A paradigm for disorders of tissue fragility. *The Journal of Clinical Investigation*, 119(7), 1784-1793.
- Couto, N., Malys, N., Gaskell, S. J., & Barber, J. (2013). Partition and turnover of glutathione reductase from *Saccharomyces cerevisiae*: A proteomic approach. *Journal of Proteome Research*, 12(6), 2885-2894.
- Dahlman-Wright, K., Cavailles, V., Fuqua, S. A., Jordan, V. C., Katzenellenbogen, J. A., Korach, K. S., et al. (2006). International union of pharmacology. LXIV. estrogen receptors. *Pharmacological Reviews*, 58(4), 773-781.
- Dalton, T. P., Dieter, M. Z., Yang, Y., Shertzer, H. G., & Nebert, D. W. (2000). Knockout of the mouse glutamate cysteine ligase catalytic subunit (gclc) gene: Embryonic lethal when homozygous, and proposed model for moderate glutathione deficiency when heterozygous. *Biochemical and Biophysical Research Communications*, 279(2), 324-329.

- Dinkova-Kostova, A. T., Fahey, J. W., Wade, K. L., Jenkins, S. N., Shapiro, T. A., Fuchs, E. J., et al. (2007). Induction of the phase 2 response in mouse and human skin by sulforaphane-containing broccoli sprout extracts. *Cancer Epidemiology, Biomarkers & Prevention : A Publication of the American Association for Cancer Research, Cosponsored by the American Society of Preventive Oncology*, 16(4), 847-851.
- Endo, H., Sugioka, Y., Nakagi, Y., Saijo, Y., & Yoshida, T. (2008). A novel role of the NRF2 transcription factor in the regulation of arsenite-mediated keratin 16 gene expression in human keratinocytes. *Environmental Health Perspectives*, 116(7), 873.
- Fuchs, E., & Green, H. (1980). Changes in keratin gene expression during terminal differentiation of the keratinocyte. *Cell*, 19(4), 1033-1042.
- Fuchs, E., & Hanukoglu, I. (1983). Unraveling the structure of the intermediate filaments. *Cell*, 34(2), 332-334.
- Genetics Home Reference (2016). Pachyonychia congenita. *U.S. National Library of Medicine*. [<https://ghr.nlm.nih.gov/condition/pachyonychia-congenita>].
- Hermanto, U., Zong, C. S., Li, W., & Wang, L. H. (2002). RACK1, an insulin-like growth factor I (IGF-I) receptor-interacting protein, modulates IGF-I-dependent integrin signaling and promotes cell spreading and contact with extracellular matrix. *Molecular and Cellular Biology*, 22(7), 2345-2365.
- International PC Consortium (2016). [[http://www.pachyonychia.org/pc\\_consortium.php](http://www.pachyonychia.org/pc_consortium.php)].

- Itoh, K., Wakabayashi, N., Katoh, Y., Ishii, T., Igarashi, K., Engel, J. D., et al. (1999). Keap1 represses nuclear activation of antioxidant responsive elements by Nrf2 through binding to the amino-terminal Neh2 domain. *Genes & Development*, 13(1), 76-86.
- Jia, D., Duan, F., Peng, P., Sun, L., Liu, X., Wang, L., et al. (2013). Up-regulation of RACK1 by TGF- $\beta$ 1 promotes hepatic fibrosis in mice. *PLoS One*, 8(3), e60115.
- Kerns, M. L., Hakim, J. M., Lu, R. G., Guo, Y., Berroth, A., Kaspar, R. L., et al. (2016). Oxidative stress and dysfunctional NRF2 underlie pachyonychia congenita phenotypes. *The Journal of Clinical Investigation*, 126(6), 2356-2366.
- Kerns, M. L., DePianto, D., Dinkova-Kostova, A. T., Talalay, P., & Coulombe, P. A. (2007). Reprogramming of keratin biosynthesis by sulforaphane restores skin integrity in epidermolysis bullosa simplex. *Proceedings of the National Academy of Sciences of the United States of America*, 104(36), 14460-14465.
- Kim, Y. H., Coon, A., Baker, A. F., & Powis, G. (2011). Antitumor agent PX-12 inhibits HIF-1 $\alpha$  protein levels through an Nrf2/PMF-1-mediated increase in spermidine/spermine acetyl transferase. *Cancer Chemotherapy and Pharmacology*, 68(2), 405-413.
- Kobayashi, A., Kang, M. I., Okawa, H., Ohtsuji, M., Zenke, Y., Chiba, T., et al. (2004). Oxidative stress sensor Keap1 functions as an adaptor for Cul3-based E3 ligase to regulate proteasomal degradation of Nrf2. *Molecular and Cellular Biology*, 24(16), 7130-7139.
- Koinuma, D., Tsutsumi, S., Kamimura, N., Taniguchi, H., Miyazawa, K., Sunamura, M., et al. (2009). Chromatin immunoprecipitation on microarray analysis of Smad2/3 binding sites

- reveals roles of ETS1 and TFAP2A in transforming growth factor beta signaling. *Molecular and Cellular Biology*, 29(1), 172-186.
- Kroger, C., Loschke, F., Schwarz, N., Windoffer, R., Leube, R. E., & Magin, T. M. (2013). Keratins control intercellular adhesion involving PKC-alpha-mediated desmoplakin phosphorylation. *The Journal of Cell Biology*, 201(5), 681-692.
- Kwak, M. K., Itoh, K., Yamamoto, M., Sutter, T. R., & Kensler, T. W. (2001). Role of transcription factor Nrf2 in the induction of hepatic phase 2 and antioxidative enzymes in vivo by the cancer chemoprotective agent, 3H-1, 2-dimethiole-3-thione. *Molecular Medicine (Cambridge, Mass.)*, 7(2), 135-145.
- Leachman, S. A., Kaspar, R. L., Fleckman, P., Florell, S. R., Smith, F. J., McLean, W. I., et al. (2005). Clinical and pathological features of pachyonychia congenita. *Journal of Investigative Dermatology Symposium Proceedings*, 10. (1) pp. 3-17.
- Lessard, J. C., & Coulombe, P. A. (2012). Keratin 16-null mice develop palmoplantar keratoderma, a hallmark feature of pachyonychia congenita and related disorders. *Journal of Investigative Dermatology*, 132(5), 1384-1391.
- Lessard, J. C., Pina-Paz, S., Rotty, J. D., Hickerson, R. P., Kaspar, R. L., Balmain, A., et al. (2013). Keratin 16 regulates innate immunity in response to epidermal barrier breach. *Proceedings of the National Academy of Sciences of the United States of America*, 110(48), 19537-19542.

- Lloyd, C., Yu, Q. C., Cheng, J., Turksen, K., Degenstein, L., Hutton, E., et al. (1995). The basal keratin network of stratified squamous epithelia: Defining K15 function in the absence of K14. *The Journal of Cell Biology*, 129(5), 1329-1344.
- Lo, R., & Matthews, J. (2013). The aryl hydrocarbon receptor and estrogen receptor alpha differentially modulate nuclear factor erythroid-2-related factor 2 transactivation in MCF-7 breast cancer cells. *Toxicology and Applied Pharmacology*, 270(2), 139-148.
- Lushchak, V. I. (2012). Glutathione homeostasis and functions: Potential targets for medical interventions. *Journal of Amino Acids*, 2012
- McGowan, K. M., & Coulombe, P. A. (1998). Onset of keratin 17 expression coincides with the definition of major epithelial lineages during skin development. *The Journal of Cell Biology*, 143(2), 469-486.
- Niture, S. K., Jain, A. K., & Jaiswal, A. K. (2009). Antioxidant-induced modification of INrf2 cysteine 151 and PKC-delta-mediated phosphorylation of Nrf2 serine 40 are both required for stabilization and nuclear translocation of Nrf2 and increased drug resistance. *Journal of Cell Science*, 122(Pt 24), 4452-4464.
- Oshimori, N., Oristian, D., & Fuchs, E. (2015). TGF- $\beta$  promotes heterogeneity and drug resistance in squamous cell carcinoma. *Cell*, 160(5), 963-976.
- Paladini, R. D., Takahashi, K., Bravo, N. S., & Coulombe, P. A. (1996). Onset of re-epithelialization after skin injury correlates with a reorganization of keratin filaments in wound edge keratinocytes: Defining a potential role for keratin 16. *The Journal of Cell Biology*, 132(3), 381-397.

- Pastore, A., Piemonte, F., Locatelli, M., Lo Russo, A., Gaeta, L. M., Tozzi, G., et al. (2001). Determination of blood total, reduced, and oxidized glutathione in pediatric subjects. *Clinical Chemistry*, 47(8), 1467-1469.
- Rugg, E. L., McLean, W. H., Lane, E. B., Pitera, R., McMillan, J. R., Dopping-Hepenstal, P. J., et al. (1994). A functional "knockout" of human keratin 14. *Genes & Development*, 8(21), 2563-2573.
- Schafer, M., Dutsch, S., auf dem Keller, U., Navid, F., Schwarz, A., Johnson, D. A., et al. (2010). Nrf2 establishes a glutathione-mediated gradient of UVB cytoprotection in the epidermis. *Genes & Development*, 24(10), 1045-1058.
- Seoane, J., Le, H., Shen, L., Anderson, S. A., & Massagué, J. (2004). Integration of smad and forkhead pathways in the control of neuroepithelial and glioblastoma cell proliferation. *Cell*, 117(2), 211-223.
- Singh, K., Connors, S. L., Macklin, E. A., Smith, K. D., Fahey, J. W., Talalay, P., et al. (2014). Sulforaphane treatment of autism spectrum disorder (ASD). *Proceedings of the National Academy of Sciences of the United States of America*, 111(43), 15550-15555.
- Smith, F. J., Liao, H., Cassidy, A. J., Stewart, A., Hamill, K. J., Wood, P., et al. (2005). The genetic basis of pachyonychia congenita. *Journal of Investigative Dermatology Symposium Proceedings*, 10. (1) pp. 21-30.
- Thornton, M., Taylor, A. H., Mulligan, K., Al-Azzawi, F., Lyon, C. C., O'Driscoll, J., et al. (2003). The distribution of estrogen receptor  $\beta$  is distinct to that of estrogen receptor  $\alpha$

- and the androgen receptor in human skin and the pilosebaceous unit. *Journal of Investigative Dermatology Symposium Proceedings*, , 8. (1) pp. 100-103.
- Trachootham, D., Lu, W., Ogasawara, M. A., Valle, N. R., & Huang, P. (2008). Redox regulation of cell survival. *Antioxidants & Redox Signaling*, 10(8), 1343-1374.
- Woodcock-Mitchell, J., Eichner, R., Nelson, W. G., & Sun, T. T. (1982). Immunolocalization of keratin polypeptides in human epidermis using monoclonal antibodies. *The Journal of Cell Biology*, 95(2 Pt 1), 580-588.
- Yang, Y., Dieter, M. Z., Chen, Y., Shertzer, H. G., Nebert, D. W., & Dalton, T. P. (2002). Initial characterization of the glutamate-cysteine ligase modifier subunit gclm(-/-) knockout mouse. novel model system for a severely compromised oxidative stress response. *The Journal of Biological Chemistry*, 277(51), 49446-49452.
- Zhang, T., Liang, X., Shi, L., Wang, L., Chen, J., Kang, C., et al. (2013). Estrogen receptor and PI3K/Akt signaling pathway involvement in S(-) equol-induced activation of Nrf2/ARE in endothelial cells. *PLoS One*, 8(11), e79075.
- Zhang, Y., Talalay, P., Cho, C. G., & Posner, G. H. (1992). A major inducer of anticarcinogenic protective enzymes from broccoli: Isolation and elucidation of structure. *Proceedings of the National Academy of Sciences of the United States of America*, 89(6), 2399-2403.

## CURRICULUM VITAE

*Rosemary G. Lu*

Home Address:  
120 N. Belnord Avenue  
Baltimore, MD 21224  
Email: [rlu16@jhu.edu](mailto:rlu16@jhu.edu)

Laboratory Address:  
615 N. Wolfe Street  
Room W8030  
Baltimore, MD 21205

### EDUCATION

- 2016      **Master of Science (ScM), Laboratory of Dr. Pierre A. Coulombe, PhD**  
Department of Biochemistry and Molecular Biology  
Johns Hopkins Bloomberg School of Public Health, Baltimore, MD  
**ScM Thesis:** Keratin 16 as a novel regulator of Nrf2 function in glabrous skin: Implications for pachyonychia congenita and its treatment  
**MHS Thesis:** Understanding the role of autoimmune regulator (AIRE) in autoimmunity through APECED and speculation of function in the periphery
- 2014      **Bachelor of Science (BS), *cum laude***  
Department of Biological Sciences  
George Washington University, Washington, DC

### AWARDS

- 2016      Spirit of Student Assembly Award  
SOURCE Champion of the Month
- 2014      Dean's List
- 2010-2014      Board of Trustee's Scholarship

### TEACHING EXPERIENCE

- 2012-2013      **Undergraduate Teaching Assistant**  
Department of Biological Sciences  
George Washington University, Washington, DC  
**Course Title:** Introductory Biology Laboratory (Dr. Harmut Doebel, PhD), 3 semesters

### PUBLICATIONS

Kerns, M. L., Hakim, J. M., **Lu, R. G.**, Guo, Y., Berroth, A., Kaspar, R. L., and Coulombe, P.A. (2016). Oxidative stress and dysfunctional NRF2 underlie pachyonychia congenita phenotypes. *The Journal of Clinical Investigation*, 126(6), 2356-2366.

Barberio, M.D., **Lu, R.**, and Hubal, M.J. (2015). Optimal Physical Activity & Exercise Following Bariatric Surgery. In Mandy Chambers (Ed.), *Bariatric Surgery: Prevalence, Complications and Impact on Quality of Life*. Hauppauge, NY: Nova Science Publishers Inc.

Fujimoto, K., Matsuura, K., Hu-Wang, E., **Lu, R.**, and Shi, Y.B. (2012). *Thyroid Hormone Activates Protein Arginine Methyltransferase 1 Expression by Directly Inducing c-Myc Transcription during Xenopus Intestinal Stem Cell Development*. *J Biol Chem*, 287(13), 10039-10050.

Sun, G., Hasebe, T., Fujimoto, K., **Lu, R.**, Fu, L., Matsuda, H., Kajita, M., Ishizuya-Oka, A., and Shi, Y.B. (2010). *Spatio-Temporal Expression Profile of Stem Cell-Associated Gene LGR5 in the Intestine during Thyroid Hormone-Dependent Metamorphosis in Xenopus laevis*. *PLoS One*, 5(10), e13605.

## PRESENTATIONS

**Lu, R.** Vive la difference: Designing a sex-specific approach for the treatment of pachyonychia congenita (PC). Presented at the Johns Hopkins Bloomberg School of Public Health Department of Biochemistry and Molecular Biology Research Retreat, Baltimore, MD (2016).

**Lu, R.**, Hakim, J.M., Kerns, M. L., Castellanos, C., Coulombe, P.A. Sex: A neglected variable in oxidative stress-associated skin biology." Presented at the Johns Hopkins Bloomberg School of Medicine Department of Dermatology Research Day, Baltimore, MD (2016).

**Lu, R.**, Kerns, M. L., Hakim, J.M., Guo, Y., and Coulombe, P.A. Defining the role of keratin 16 in wound-associated oxidative stress." Presented at the Johns Hopkins Bloomberg School of Public Health Delta Omega Scientific Poster Competition, Baltimore, MD (2016).

**Lu, R.**, Sevilla, S., Nadler, E.P., and Hubal, M.J. FTO genotype is associated with ALT levels in obese adults. Presented at the George Washington University Research Days, Washington, DC (2014).